ANESTHESIOLOGY®

Journal Pre-proof

Effect of fractalkine signaling on neuroinflammation and neuropathic pain-like behavior in mice

Qingyuan Fan, MD, PhD, Jihye Kim, PhD, Jie Zhang, MD, PhD, Quanri Zhang, PhD, Mi-Hyun Hwang, PhD, Jing Li, MD, Fei Li, MD, Yan Yin, MD, Yingchun Han, MD, Karan Shah, MS, Riqiang Yan, PhD, Jianguo Cheng, MD, PhD.

DOI: https://doi.org/10.1097/ALN.0000000000006257

To appear in: Anesthesiology

Submitted for publication: January 12, 2026

Accepted for publication: July 02, 2026

Please cite this article as: Fan Q, Kim J, Zhang J, Zhang Q, Hwang M-H, Li J, Li F, Yin Y, Han Y, Shah K, Yan R, Cheng J: Effect of fractalkine signaling on neuroinflammation and neuropathic pain-like behavior in mice. Anesthesiology. 2026; https://doi.org/10.1097/ALN.0000000000006257

Anesthesiology Publish Ahead of Print

DOI: 10.1097/ALN.0000000000006257

Effect of fractalkine signaling on neuroinflammation and neuropathic pain-like behavior in mice

Qingyuan Fan, MD, PhD[1], Jihye Kim, PhD[1], Jie Zhang, MD, PhD[1], Quanri Zhang, PhD[1], Mi-Hyun Hwang, PhD,[1] Jing Li, MD[1], Fei Li, MD[1], Yan Yin, MD,[1] Yingchun Han, MD,[2] Karan Shah, MS[3], Riqiang Yan, PhD[4], Jianguo Cheng, MD, PhD[1*]

[1]*Departments of Pain Management and Neurosciences*

Neurological Institute, Cleveland Clinic,

[2]*Department of Inflammation and Immunity, Cleveland Clinic.*

[3]*Department of Quantitative Health Sciences, Cleveland Clinic*

9500 Euclid Avenue, Cleveland, Ohio, USA 44195

[4]*Department of Neuroscience, University of Connecticut.*

263 Farmington Avenue, Farmington, CT 06030-3401

[*] **Corresponding author:** Jianguo Cheng, MD, Ph.D. Professor of Anesthesiology and Director of the Cleveland Clinic Consortium for Pain Departments of Pain Management and Neurosciences, Cleveland Clinic 9500 Euclid Avenue/C25 Cleveland, Ohio, 44195 Phone: +1 216 337 1509 Email: chengj@ccf.org

Clinical Trial Registration: not applicable

Prior Presentations:

1. Cheng J, Fan Q, Kim J, Zhang J. Enhancing fractalkine signaling attenuates neuropathic pain through dual pathways. ***International Association for the Study of Pain 20th World Congress*** *on Pain*, August 5 – 9, 2024, Amsterdam, Netherlands

2. Cheng J, Fan Q, Kim J, Zhang J. Enhancing fractalkine signaling normalizes the expression of CCI-induced differentially expressed genes and attenuates neuropathic pain in mice. ***Society for Neuroscience*** **Annual Meeting** 2023. November 11-15, Washington, DC.
3. Fan Q, Li J, Li F, Yin Y, Cheng J. Enhancing fractalkine signaling attenuates neuroinflammation and neuropathic pain induced by chronic constriction nerve injury in mice. ***Society for Neuroscience*** **Annual Meeting** 2022. November 12-16, San Diego, CA

Word and Element Counts:

- Abstract: 274
- Introduction: 400
- Discussion: 1627
- Number of references: 79
- Figures: 8
- Tables: 0
- Appendices: supplemental figures 5.
- Supplemental digital content files: 1

Abbreviated Title: Fractalkine signaling attenuates neuropathic pain

Summary Statement: not applicable

Funding Statement: The work is supported by the following grants:

- National Institutes of Health NIH/NINDS/1UG3NS127258-01A1 UG3/UH3 (JC)
- Department of Defense W81XWH-11-1-0672.10669042 (JC)
- Lisa Dean Moseley Foundation (LDMF 0920JC, 1909JC, 1812JC, and 1709JC)
- 2025 Falk Medical Research Trust Catalyst Award from Dr. Ralph and Marian Falk Medical Research Trust Bank of America, Private Bank, Trustee (JC)

- Cleveland Clinic Pain Management Innovations Fund #T56629 (JC).
- Cleveland Clinic Pain Management Treasury Fund #I111674 (JC)

Conflict of interest: Jianguo Cheng has declared the following COI statements:

MD Anderson Cancer Center, Grand Round lecture honorarium, 2025.

Vertex Pharmaceuticals Inc. Chronic pain advisory board, 2025.

Boston Scientific Inc, royalty payment for patent license for a medical device he invented, 2017-2026.

Oxford University Press, royalty for a textbook as Editor, 2019-2026.

Nature Springer, royalty for two textbooks as editor, 2018-2026.

Abbreviations and Acronyms

ANOVA, Analysis of Variance

Arg1, Arginase-1

Cat-S, Cathepsin S

CCI, Chronic constriction injury

CCL2, Chemokine (C–C motif) ligand 2

CCR2, Chemokine C-C motif receptor 2

CNS, Central nervous system

CREB, Cyclic adenosine monophosphate response element-binding protein

CX3CL1, Fractalkine

CX3CL1-FL, full-length CX3CL1

CX3CL1-Tg, Transgenic CX3CL1 mouse model

DEGs, Differentially-expressed genes

DRG, Dorsal root ganglion

ERK, Extracellular signal-regulated kinase

FACS, Fluorescence-activated cell sorting

FC, Fold change

FDR, False discovery rate

GFP, Green fluorescent protein

GO, Gene Ontology

GSEA, Gene Set Enrichment Analysis

ICAM-1, Intracellular adhesion molecule-1

IFN-γ, Interferon γ

IL, Interleukin

iNOS, Inducible nitric oxide synthase

IPA, Ingenuity Pathway Analysis

KO, Knock out

LPS, Lipopolysaccharide

MAPK, Mitogen-activated protein kinase

MCP-1, Monocyte chemoattractant protein-1

MMP, Metalloprotease

NF-κB, Nuclear factor-κB

NP, Neuropathic pain

PCA, Principal Component Analysis

PI3K, Phosphatidylinositide 3-kinase

PNS, Peripheral nervous system

PWL, Paw withdrawal latency

PWT, Paw withdrawal threshold

RNA-Seq, RNA sequencing

SC, Spinal cord

SN, Sciatic nerve

STAT3, Signal transducer and activator of transcription 3

TGF-β, Transforming growth factor β

TNF-α, Tumor necrosis factor-alpha

TREM, Triggering receptors expressed on myeloid cells

VCAM-1, Vascular cell adhesion molecule-1

ABSTRACT

Background: Neuropathic pain is the most prevalent and incapacitating form of chronic pain. Understanding its pathogenesis at the cellular and molecular levels is crucial to guide the development of new therapeutics. A major controversy has been on the roles of Fractalkine (CX3CL1) signaling between neurons and immune cells in the pathogenesis of neuropathic pain. In this study, we investigated two distinct pathways of CX3CL1 signaling in the pathogenesis of neuropathic pain, namely the CX3CR1-dependent pathway and the TGF-β/Smad2/3-dependent pathway.

Methods: Neuropathic pain-like behavior was induced in mice using the sciatic nerve chronic constriction injury (CCI) model. Experiments were performed in wild-type, CX3CR1-knockout, and CX3CL1-transgenic mice to examine distinct CX3CL1 signaling pathways. Microglia and macrophage activation, CX3CL1 processing, TGF-β/Smad2/3 signaling, and inflammatory cytokine expression were assessed using molecular and immunohistochemical techniques. Behavioral assays quantified mechanical allodynia and thermal hyperalgesia, and transcriptomic analyses evaluated neuroimmune gene expression changes following CCI injury and CX3CL1 signaling manipulations.

Results: CCI of the sciatic nerve led to activation of microglia and macrophages, cleavage and consumption of full-length CX3CL1, and a decrease in the expression of its downstream TGF-β family proteins. Deletion of CX3CR1 in CX3CR1-knockout mice exacerbated CCI-induced neuroinflammation. Conversely, overexpression of CX3CL1 in CX3CL1-Tg mice significantly enhanced TGF-β/Smad2/3 signaling, reduced pro-inflammatory cytokines, inhibited microglia activation, and alleviated CCI-induced hyperalgesia. Moreover, CX3CL1 overexpression

effectively reversed the CCI-induced differentially expressed genes (DEGs) and neuro-immune responses.

Conclusions: These findings demonstrate that enhancing CX3CL1 signaling effectively mitigates neuroinflammation and alleviates neuropathic pain-like behavior, likely through CX3CL1 signaling between neuronal and immune cells via two distinct pathways: the CX3CR1-dependent pathway mediated through the CX3CL1 N-terminus, and the TGF-β-dependent pathway mediated through the CX3CL1 C-terminus.

INTRODUCTION

Neuropathic pain (NP) affects 7-10% of the global population and is the most debilitating form of pain.[1] It often results from lesions or disease of the somatosensory nervous systems.[2] Given the limited effectiveness of current treatments for NP, elucidating its cellular and molecular mechanisms is essential for informing the development of novel therapeutic strategies. Neuro-immune communications through signaling molecules, such as cytokines and chemokines, play a central role in neuroinflammation that underlies peripheral and central sensitizations of pain.[3,4] Despite extensive investigation, the role of neuron–microglia crosstalk mediated by fractalkine (CX3CL1) in the pathogenesis of NP remains highly controversial.[5-8]

CX3CL1 is constitutively expressed in neurons, predominantly in a membrane-bound form.[9,10] Proteolytic ectodomain shedding releases a soluble N-terminal fragment containing the C-X-X-X-C motif, which binds its exclusive G protein–coupled receptor, CX3CR1.[11,12] on microglia and macrophages.[13] We recently demonstrated that the membrane-bound CX3CL1 C-terminus translocates to the neuronal nucleus and activates TGF-β/Smad2/3 signaling in the 5XFAD mouse model of Alzheimer's disease,[23] although its role in neuropathic pain remains unknown. Together, the N- and C-terminal domains may differentially regulate neuron–glia crosstalk and cellular function in a context-dependent manner.[14] Notably, existing NP studies have focused exclusively on N-terminal, CX3CR1-dependent mechanisms. Several studies suggest that CX3CL1/CX3CR1 signaling mediated by the CX3CL1 N-terminus contributes to NP by promoting microglia activation and neuroinflammation.[5,6,15,16] However, conflicting evidence shows that CX3CR1-knockout (KO) mice exhibit worsened allodynia after spared nerve injury, and that intra-neural CX3CL1 administration delays allodynia development in wild-type animals.[17] Consistently, therapeutic inhibition of this pathway has failed to alleviate NP.

Moreover, growing evidence indicates that CX3CL1/CX3CR1 signaling exerts anti-inflammatory and neuroprotective effects in neurodegenerative diseases such as Alzheimer's and amyotrophic lateral sclerosis.[18,19] Together, these findings underscore the unresolved and context-dependent roles of this pathway in NP pathogenesis.[6,20]

In this study, we investigated the role of CX3CL1 signaling in NP induced by chronic constriction injury (CCI) of the sciatic nerve in mice, evaluating both N-terminus–mediated soluble signaling and C-terminus–mediated membrane-bound signaling. We hypothesized that either inhibition or enhancement of CX3CL1 signaling would regulate neuroinflammation and NP. To assess the role of CX3CR1-dependent CX3CL1 signaling in NP, we used CX3CR1 knockout ($CX3CR1^{GFP/GFP}$) mice. To examine the effects of enhanced CX3CL1 signaling on NP and neuroinflammation, we generated a transgenic CX3CL1 mouse model (CX3CL1-Tg) that overexpresses full-length CX3CL1 (CX3CL1-FL) in neuronal cells of the central and peripheral nervous systems under the control of a prion promoter.

MATERIALS AND METHODS

All experimental protocols were approved by the Institutional Animal Care and Use Committee of the Lerner Research Institute in compliance with the guidelines established by the Public Health Service Guide for the Care and Use of Laboratory Animals.

Animals

CX3CR1 KO mice ($CX3CR1^{GFP/GFP}$) expressing EGFP in microglia, macrophages/monocytes, dendritic cells, and NK cells under the control of the endogenous *CX3CR1* locus were purchased from the Jackson Laboratory. CX3CL1-FL transgenic (CX3CL1-Tg) mice were generated in our labs as previously described[21]. Specifically, the transgenic construct includes a neuronally driven CX3CL1 overexpression cassette fused with an HA

epitope tag, enabling detection of transgene expression. The HA tag is selectively expressed in neurons in parallel with CX3CL1 overexpression and is not present in endogenous protein. Accordingly, HA immunoreactivity was used as a surrogate marker to identify cells overexpressing CX3CL1 in our immunohistochemistry experiments. All the mice were bred onto the C57BL6/J background (6 to 8 backcrosses). CX3CR1$^{GFP/+}$ and CX3CL1-Tg/CX3CR1$^{GFP/+}$ mice were generated by crossing CX3CR1$^{GFP/GFP}$ and CX3CL1-Tg mice and by subsequent intercrossing of heterozygous F1 animals in our lab. The mice were group-housed (4–5/cage) in standard cages in a colony room maintained on a 12-hour reversed light/dark cycle. All mice had continuous access to food and water throughout the study. Mice were handled and adapted to the testing environment for 1 week before the initiation of the experiments.

CCI was performed as reported in our previous publications, with minor modifications specific to mice.[22] Briefly, under anesthesia, the right sciatic nerve was exposed by making a skin incision and cutting through the connective tissue between the gluteus superficialis and biceps femoris muscles. Three chromic gut ligatures were tied loosely around the sciatic nerve at 1 mm intervals to just occlude but not arrest epineural blood flow. The incision was closed with staples in the skin. The animal was then allowed to recover from surgery 24 hours before mechanical pain hypersensitivity testing. All behavioral testing procedures were conducted between 08:00 and 13:00 h. Both male and female mice were used in balanced numbers.

Mechanical and Thermal Sensitivity Testing

All behavioral measurements were performed in the Behavior Core Facility by experienced experimenters blinded to the experimental procedure between 10 am and 4 pm. The sensitivity to noxious stimulation was determined by measuring the paw withdrawal thresholds (PWTs) in response to mechanical stimulation and paw withdrawal latency (PWL) in response to

thermal stimulation to the hind paws. The mice were handled and habituated to the behavioral testing environment to minimize stress. For mechanical testing, animals were placed in individual 8 × 8 × 18 cm plastic boxes on an elevated metal wire mesh floor and allowed to acclimate for at least 30 min before the test. Mechanical sensitivity was tested using von Frey sensory evaluator filaments (Stoelting, Wood Dale, IL, USA) that were applied to the plantar surface of the hind paws in ascending order of force (0.008 – 6 grams) until the filament bent and was held there for ~3 seconds or until an acute paw withdrawal response took place. Upon a paw withdrawal response, the filaments were applied in descending order, beginning with the next thinner filament until there was no withdrawal response. The threshold was the thinnest filament to evoke a paw withdrawal response. The procedure was repeated three times at 5-minute intervals to avoid sensitization, and the withdrawal thresholds were averaged and recorded (mean ± SD).

For thermal testing, mice were habituated individually in polyvinyl boxes (10 × 10 × 10 cm) placed on glass heated to 25°C for at least 30 min prior to behavioral assessment using the Hargreaves Test (Plantar Analgesia Meter, IITC, CA, USA). The radiant heat light source (intensity 15%) was focused on the plantar surface of each hind paw, and the time taken for the mouse to withdraw the paw was recorded, with a cut-off of 20 s to prevent tissue damage. The mean time to withdrawal was determined from the average of 3 tests, separated by at least 1 min.

RT-PCR

Total RNA was isolated from the fresh sciatic nerve, DRG, and spinal cord tissues using the RNeasy Plus Universal Mini kit (73404; Qiagen) according to the manufacturer's instructions. The concentration of RNA was measured using a Nanodrop-1000 (Nanodrop Technologies, Wilmington, DE, USA), and sample purity was evaluated by determining the

absorbance ratio at 260 and 280 nm, which was between 1.9 and 2.1. Complementary DNA was synthesized from total RNA using a High-Capacity cDNA Reverse Transcription kit (4368814; Applied Biosystems) and Simpliamp Thermal Cycler (Thermo Fisher Scientific) according to the manufacturer's cycling parameters. The expression of reported genes of TNF-α, IL-1β, IL-6, CX3CL1, and CX3CR1 was analyzed using TaqMan Gene Expression Assays (Thermo Fisher). β-actin was used as an endogenous control in the reaction. Delta Ct values were used to determine relative expression changes ($2^{-\Delta\Delta}$CT) and were presented as fold change (FC).

Western blotting

Total protein was extracted from freshly dissected mouse tissue in RIPA lysis buffer (Thermo Fisher) supplemented with 1X Halt protease and phosphatase inhibitor cocktails (Thermo Fisher). Equal amounts of protein (30 or 50 µg) were resolved on an Invitrogen Nu-PAGE 4-12% Bis-Tris gel (Thermo Fisher Scientific) and transferred onto an Invitrogen nitrocellulose membrane (Thermo Fisher Scientific). At least four mice from each genotype group were used for Western blot analysis. Membranes were blocked in 5% non-fat dry milk in tris-buffered saline with Tween-20 (TBST) for 1 hour at room temperature followed by incubating membrane overnight at 4°C in the following primary antibodies: Fractalkine (C-20) (Catalog # sc-7225, RRID: AB_2087136), HA (catalog # 11867423001, Roche; RRID: AB_ 390918), TGF-β1 (catalog # 21898-1-AP, RRID: AB_2811115), TGF-β2 (catalog # sc-374659, RRID: AB_10988781), TGF-β3 (catalog # sc-166833, RRID: AB_2303246), p-Smad2 (catalog # 3104; RRID: AB_390732), p-Smad3 (catalog # 9520; RRID: AB_2193207), Smad2/3 (catalog # 8685; RRID: AB_10889933), β-actin (catalog # A5441; Sigma-Aldrich; RRID: AB_476744). HRP-conjugated secondary antibodies were used and visualized using enhanced chemiluminescence (Thermo Fisher Scientific). Chemiluminescence bands were detected with

Clarity Western ECL substrate (Bio-Rad Laboratories, Hercules, CA) and imaged using a Bio-Rad ChemiDocMP and analyzed and quantified using Image J software (ver. 5).

Cytokine/Chemokine multiplex assay

The lumbar segments of the spinal cord were dissected from WT and CX3CR1$^{GFP/GFP}$ mice. Tissues were homogenized in a lysis buffer containing protease and phosphatase inhibitors. Tissue homogenates were mixed at 4 °C for 20 min before centrifugation at 11,000 rpm at 4 °C for 20 min. The supernatant was isolated from the pellet before a second centrifugation to obtain a completely clear supernatant. Protein concentrations were determined by BCA Protein Assay (Pierce). All the samples were analyzed using Mouse Cytokine Array/Chemokine Array 31-Plex (MD31) (EVE Technologies, Calgary, AB, Canada) according to the manufacturer's protocols.

Immunohistochemical staining

Immunohistochemical staining experiments were performed using standard methods. Briefly, mice were sacrificed by intracardiac perfusion with ice-cold PBS, followed by 4% PFA solution under deep anesthesia (Phenobarbital Sodium). The lumbar segment of the spinal cord (L4-6), the DRGs, and the sciatic nerve of both sides were rapidly dissected and post-fixed in 4% PFA for 24 hours and immersed in 30% sucrose for 48 hours at 4°C. Afterward, 10-um-thick tissues of the DRG and the sciatic nerve were cut on a cryostat machine (Leica Microsystems) and mounted on the slides. 30-um-thick coronal sections of the spinal cord were cut and kept in cryostorage buffer at −20 °C. Sections were permeabilized with 0.3% Triton X-100 for 30 min. After being rinsed in PBS three times to remove detergent, the sections were heated by microwave in 0.05 M citrate-buffered saline, pH 6.0, for 5 min, blocked with 5% normal goat serum, and incubated with individual primary antibodies at a 1:500 dilution (HA). After washing

with PBS three times, sections were incubated with secondary antibodies conjugated with Invitrogen Alexa Fluor 568 (Thermo Fisher Scientific).

Quantification of immunoreactivity

Quantification of the percentage area occupied by immunoreactivity of $CX3CR1^{+}$ cells in the dorsal horn (number per unit area) was performed in a blinded fashion on serial sections of each mouse. Briefly, serial 20x pictures of the superficial area of the lumbar spinal cord dorsal horn were captured by confocal microscopy and used for quantification. Digitized images were analyzed with Image-Pro 7 software. A thresholding procedure was established to determine the proportion of immunoreactive areas within each fixed field of view. These parameters were then held constant for each set of images obtained at equal objectives and light intensities. The data represent the mean immunoreactivity area in the spinal cord dorsal horn.

RNA sequencing (RNA-Seq) analysis

RNA-Seq analysis was performed through the Genewiz Company, blinded to the experimental conditions. Briefly, total RNA (tRNA) samples were quantified using a Qubit 2.0 Fluorometer (Life Technologies, Carlsbad, CA, USA), and RNA integrity was checked using Agilent TapeStation 4200 (Agilent Technologies, Palo Alto, CA, USA). More than five hundred nanograms of tRNA per sample were used to construct sequencing libraries (n=1 mouse/sample) using the NEBNext Ultra RNA Library Prep Kit for Illumina (New England Biolabs Inc., Ipswich, MA, USA). The sequencing libraries were validated on the Agilent TapeStation and quantified by using the Qubit 2.0 Fluorometer (Invitrogen, Carlsbad, CA) as well as by quantitative PCR (KAPA Biosystems, Wilmington, MA, USA). The sequencing libraries were clustered and loaded on the Illumina HiSeq instrument (4000 or equivalent). The samples were sequenced using a 2x150bp Paired-End (PE) configuration. Image analysis and base calling were

conducted by HiSeq Control Software (HCS). Raw sequence data (bcl files) generated from Illumina HiSeq were converted into fastq files and de-multiplexed using Illumina's bcl2 fastq 2.17 software. After investigating the quality of the raw data, the sequence read was trimmed to remove possible adapter sequences and nucleotides with poor quality using Trimmomatic v.0.36. The trimmed reads were mapped to the Mus musculus reference genome available on ENSEMBL using the STAR aligner v.2.5.2b. BAM files were generated because of this step. Unique gene hit counts were calculated by using Feature Counts from the Subread package v.1.5.2. Unique reads that fall within exon regions were counted. After the extraction of gene hit counts, the gene hit counts table was used for downstream differential expression analysis. Comparisons of gene expression between the groups of samples were performed using DESeq2. The Wald test was used to generate p-values and Log2 fold changes. Genes with adjusted p-values < 0.05 and absolute log2 fold changes > 1 were called differentially expressed genes for each comparison. Genes with differential expressions between groups were then included in Gene Ontology (GO) and Ingenuity Pathway Analysis (IPA) to infer their functional roles and relationships. GO analysis for enriched GO biological processes in each set of differentially enriched genes identified by DESeq2 was performed using GSEA (Gene Set Enrichment Analysis) [PMID: 16199517, 12808457]. The International Union of Basic and Clinical Pharmacology database (http://www.guidetopharmacology.org) was used to assign categories to gene products.

Quantification and Statistical Analysis

The paw withdrawal threshold (PWT) to mechanical stimulation and paw withdrawal latency (PWL) to thermal stimulation were expressed as mean ± SD. Based upon having 90% power to detect differences of 2 SD or more between groups at an overall 0.05 significance level,

the calculated sample size for each group is 14. To allow comparisons between male and female animals with sufficient sample sizes, we used 20 animals (10 male and 10 female) in each of the four groups. A randomization process was employed to ensure unbiased allocation of mice to the 4 different groups. Computer-generated random numbers (Excel) were utilized for this purpose.

Immunoreactivity was expressed as mean ± SD. Quantifications were performed from at least three independent experiments and in a blinded fashion. Student T-tests were used for comparisons between the two groups. One-way or two-way repeated-measures analysis of variance (ANOVA) for multiple comparisons, followed by paired comparisons with Bonferroni corrections. ANOVA was followed by Tukey's multiple comparison tests for immunohistochemistry analysis. GraphPad Prism was used for all the analyses. $P<0.05$ was considered statistically significant.

The assumption of normality was formally evaluated prior to statistical testing using the Kolmogorov–Smirnov normality test. We used the Wilcoxon/Mann-Whitney Test to compare groups when the data did not follow a normal distribution.

RESULTS

Chronic constriction injury activated CX3CR1^{+} immune cells and decreased CX3CL1-FL and TGF-β family proteins

CCI of the sciatic nerve activated microglia in the CNS and monocytes/macrophages in the PNS. Replacing one (or both) Cx3cr1 alleles with GFP enables specific visualization of microglia, monocytes, and dendritic cells in the nervous system.[23,24] CX3CR1 expression was increased in microglia in the spinal cord and macrophages in the DRG and sciatic nerve in heterozygous CX3CR1-GFP knock-in mice (CX3CR1$^{GFP/+}$) (**Fig. 1**). This microglial activation was evident by Day 3 post-CCI, peaking between Days 7 and 14 and persisting to Day 28 (**Fig.**

1A-B), as indicated by increased GFP fluorescence intensity and elevated CX3CR1 transcription levels in the spinal cord and the sciatic nerve (**Fig. S1, https://links.lww.com/ALN/E655**). Simultaneously, CX3CL1-FL and TGF-β proteins decreased across the spinal cord, DRG, and sciatic nerve. Notably, CX3CL1-FL levels were lowest in the spinal cord by Days 7–14 post-CCI, recovering partially after Day 21 **(Fig. 1C-D)**, driven by increased proteolytic cleavage rather than reduced transcription (**Fig. S1, https://links.lww.com/ALN/E655**). RNA-Seq analysis of the sciatic nerve at post-CCI Day 28 highlighted elevated proteolytic enzyme expressions (Cathepsins, ADAM 10, ADAM 17, and MMP 9) (**Fig. S2, https://links.lww.com/ALN/E655**), supporting enhanced CX3CL1 cleavage to release the soluble N-terminus and the membrane-bound C-terminus in neuronal cells. This reduction in TGF-β signaling proteins suggests compromise of their neuroprotective and anti-inflammatory effects.

CX3CL1-FL and TGF-β family protein expressions were distinct between the spinal cord and the DRG/sciatic nerve (**Fig. 1E-G**). These proteins showed significant reductions on both sides of the spinal cord during peak microglial activation, occurring between post-CCI Days 7–14. In contrast, their expression was decreased only on the ipsilateral side of the sciatic nerve and DRG. Notably, CX3CL1 and CX3CR1 expression levels were significantly higher in the spinal cord compared to the DRG and the sciatic nerve in WT mice (**Fig. S1, https://links.lww.com/ALN/E655**), consistent with robust neuron-microglia communication within the spinal cord following CCI. The weak CX3CL1-fl bands in the DRG and sciatic nerve (**Fig. 1E**) reflect a limited amount of tissue available from single DRG or sciatic nerve samples. Direct comparisons between genotype groups revealed increased expression of CX3CL1 and TGF-β in the spinal cord of CX3CL1 knockout animals compared to wild-type controls (two-

way ANOVA). This pattern was observed in both sham and CCI conditions across the ipsilateral and contralateral spinal cord tissues (**Fig 2F-G**).

Deletion of CX3CR1 exacerbated chronic constriction injury-induced neuroinflammation

CCI-induced microglial activation was enhanced and prolonged in CX3CR1 knockout (KO) ($CX3CR1^{GFP/GFP}$) mice, compared to $CX3CR1^{GFP/+}$ mice (**Fig. 2A-B**). GFP intensity of the lumbar spinal cord was significantly higher, particularly on the ipsilateral side, in $CX3CR1^{GFP/GFP}$ mice, compared to $CX3CR1^{GFP/+}$ mice at post-CCI Days 7 through 28 (**Fig. 2B**). Similarly, activation of macrophages/monocytes ($CX3CR1^{+}$ cells in the DRG and the sciatic nerve) was enhanced and prolonged in CX3CR1 KO mice, compared to $CX3CR1^{GFP/+}$ mice (data not shown). In addition, proinflammatory cytokine/chemokine (IL-1β, IL-1α, IFN-γ, and MIP-1) and anti-inflammatory cytokines (e.g., IL-10) were increased by many folds in CX3CR1 KO mice (**Fig. S3, https://links.lww.com/ALN/E655**). Thus, CCI led to exacerbated neuroinflammation in the CNS and PNS in CX3CR1 KO mice.

CX3CL1-FL protein levels in the spinal cord were approximately threefold higher in CX3CR1 KO mice than in WT and $CX3CR1^{GFP/+}$ mice (**Fig. 2C-D**), indicating accumulation of CX3CL1-FL in the absence of CX3CR1. TGF-β family proteins were also significantly increased in CX3CR1 KO mice compared to WT mice (**Fig. 2E-G**), consistent with increased C-terminus signaling consequent to proteolytic cleavage of CX3CL1-fl. Following CCI, CX3CL1-FL and TGF-β family protein levels were significantly reduced bilaterally in the spinal cord compared with sham controls in both WT and CX3CR1 KO mice (**Fig. 2E–G**). In WT mice, CCI reduced CX3CL1-FL and TGF-β family protein levels on the ipsilateral side relative to the contralateral side. In contrast, CX3CR1 KO mice showed increased ipsilateral levels, consistent

with injury-induced accumulation of CX3CL1-FL and TGF-β family proteins in the absence of CX3CR1-mediated signaling.

Neuronal CX3CL1 overexpression enhanced TGF-β/Smad2/3 signaling and reduced neuroinflammation

We generated a novel transgenic mouse model (CX3CL1-Tg), in which full-length CX3CL1 is overexpressed in neurons under the control of a prion promoter, enabling investigation of its role in neuroinflammation and NP. CX3CL1-Tg mice were crossed with $CX3CR1^{GFP/GFP}$ mice to generate CX3CL1-Tg/$CX3CR1^{GFP/+}$ mice, allowing targeted investigation of CX3CL1 signaling effects on microglia and macrophages ($CX3CR1^{+}$ cells). At post-CCI Day 7, these mice showed markedly reduced microglial activation on the ipsilateral side of the spinal cord compared to $CX3CR1^{GFP/+}$ and CX3CR1 KO ($CX3CR1^{GFP/GFP}$) mice, where microglial activation was most pronounced (**Fig. 3A**-**B**).

At post-CCI day 7, CCI significantly reduced CX3CL1, TGF-β, and Smad family protein levels in the ipsilateral spinal cord, DRG, and sciatic nerve of $CX3CR1^{GFP/+}$ mice (**Fig. 3C**-**E**). In contrast, CX3CL1-Tg mice showed more than a twofold increase in CX3CL1-FL, TGF-β, and Smad proteins in the DRG neurons and the sciatic nerve, consistent with our previous reports.[21,25] These increases were less pronounced in the spinal cord, suggesting more robust proteolytic cleavage of CX3CL1-FL in this region (**Fig. 3D–E**). Given that Smad2/3 phosphorylation and nuclear translocation are essential for TGF-β receptor signaling,[21,25] these results underscore the neuroprotective and anti-inflammatory effects of enhanced CX3CL1–TGF-β/Smad signaling in attenuating NP.

Neuronal overexpression of CX3CL1 markedly attenuated the proinflammatory cytokine response induced by CCI. In WT and CX3CR1 KO mice, CCI triggered a robust upregulation of TNF-α, IL-1β, and IL-6 levels in the spinal cord and ipsilateral sciatic nerve, with TNF-α and IL-6 increasing by several hundredfold and IL-1β by several thousandfold (**Fig. 4A–B**). CX3CR1 KO mice exhibited elevated expression of proinflammatory cytokines in the spinal cord and sciatic nerve compared with WT mice, likely to reflect loss of CX3CR1-mediated scavenging and down-regulation of inflammatory signaling. This inflammatory surge peaked between 1 and 7 days post-injury and persisted for more than 8 weeks. Similar, albeit less pronounced, changes were observed in the DRG (data not shown). In contrast, CX3CL1-Tg mice exhibited more than a 70% reduction in cytokine expression within the first two weeks and greater than a 90% reduction thereafter. The duration of the inflammatory response was shortened to approximately 4 weeks in CX3CL1-Tg mice from more than 8 weeks in WT mice.

Neuronal CX3CL1 overexpression alleviated chronic constriction injury-induced neuropathic pain-like behaviors and elevated the expression of TGF-β family proteins in the sciatic nerve

Baseline paw withdrawal thresholds (PWTs), assessing mechanical allodynia using von Frey filaments, and paw withdrawal latencies (PWLs), assessing thermal hyperalgesia using the Hargreaves method, did not differ significantly among WT, $CX3CR1^{GFP/+}$, and CX3CL1-Tg mice, indicating that neuronal overexpression of CX3CL1-FL does not alter nociceptive sensitivity under physiological conditions (data not shown). Following CCI, mechanical and thermal pain thresholds were significantly elevated in CX3CL1-Tg mice compared with WT controls at all post-injury time points, with the greatest effect observed from post-CCI day 14 through day 56 (**Fig. 5A–D**). These effects were consistent in both male and female mice, with

no evidence of sex-dependent differences in the analgesic effects of CX3CL1-mediated signaling.

In CX3CL1-Tg mice, CCI induced a marked reduction in CX3CL1-FL protein levels in the sciatic nerve immediately after injury (post-CCI day 1). This reduction persisted for approximately two weeks and gradually recovered over the subsequent two weeks (**Fig. 5E–F**). The early decline is most likely attributable to increased proteolytic cleavage and consumption of CX3CL1-FL, as evidenced by a concomitant increase in the CX3CL1 C-terminus at post-CCI day 1. The later recovery phase appears to be driven primarily by increased production of CX3CL1-FL. Notably, proteolytic cleavage and consumption of CX3CL1-FL remained elevated during the recovery phase, as indicated by sustained increases in the C-terminus, most prominently from week 3 post-CCI onward. In parallel, TGF-β family protein levels increased following a similar temporal pattern. Importantly, enhanced CX3CL1 signaling through the C-terminus–TGF-β pathway coincided with the onset and maintenance of the analgesic effects observed in CX3CL1-Tg mice (**Fig. 5A–D**). Also, activation of TGF-β-Smad2/3 signaling may ameliorate pain and cartilage degradation of osteoarthritis.[26] Collectively, these findings suggest that augmented CX3CL1 signaling attenuates NP likely through both CX3CR1-dependent mechanisms and CX3CR1-independent, TGF-β–mediated pathways. The latter appears to be mediated by coordinated signaling involving the membrane-bound CX3CL1 C-terminus, TGF-β, Smad2/3, and Hedgehog pathways, leading to suppression of neuroinflammation and improvement of neuronal function, particularly during the late phase of NP. These processes are likely localized to sciatic nerve fibers and their DRG cell bodies, consistent with our previous findings that neurons express CX3CL1-FL, the CX3CL1 C-terminus, and TGF-β proteins in CX3CL1-Tg mice.[21,25,27]

Neuronal CX3CL1 overexpression significantly normalized chronic constriction injury-induced differentially expressed genes (DEGs) involved in immune and neuronal functions.

CCI induced distinct differentially expressed genes (DEGs) in the injured sciatic nerve of both WT and CX3CL1-Tg mice. RNA sequencing was performed at post-CCI day 28, a time point chosen because robust and sustained analgesic effects were observed in CX3CL1-Tg mice from day 3 through day 56 and beyond (**Fig. 5**). The injured sciatic nerve was selected for transcriptomic analysis to maximize specificity to CCI and to focus on molecular changes occurring directly at the site of injury. While analysis of the sciatic nerve enables focused assessment of injury-site molecular changes relevant to NP, we recognize that this tissue comprises multiple cell types, including axons, Schwann cells, and infiltrating immune cells, which contribute to the overall transcriptomic profile. Because bulk RNA-sequencing was performed, the observed gene expression changes reflect composite signals from heterogeneous cell populations and cannot be attributed specifically to neuronal CX3CL1.

High data quality and reproducibility across the four experimental groups were confirmed by principal component analysis (PCA) and sample correlation analysis (**Fig. 6A**). In WT mice, CCI induced 5,882 DEGs (FDR-false discovery rate < 0.05, $|\log_2$ fold change$| > 1$) in the injured sciatic nerve compared with controls (**Fig. 6B–C**), of which 3,224 (52.5%) were upregulated and 2,658 (47.5%) were downregulated. Downregulated DEGs were significantly enriched in pathways related to synaptic transmission, synaptic organization, axonal outgrowth, and neuronal function (**Fig. 6E**). In contrast, upregulated DEGs showed significant enrichment in immune-related biological processes, including cytokine- and chemokine-mediated signaling and immune cell activation, as revealed by Gene Ontology analysis (**Fig. 6E**). These upregulated genes included key intracellular signaling molecules implicated in NP, such as Src family kinases,

phosphatidylinositide 3-kinase (PI3K/Akt), mitogen-activated protein kinase (MAPK/ERK), nuclear factor-κB (NF-κB), and cAMP response element–binding protein (CREB). Ingenuity Pathway Analysis identified IL-1β, IL-1α, TNF, IFN-γ, IL-6, and IL-17A as dominant upstream regulators driving the enhanced immune responses (**Fig. 6F**). Notably, anti-inflammatory cytokines, including IL-10 and TGF-β1, were also significantly upregulated (**Fig. S2, https://links.lww.com/ALN/E655**), indicating a coordinated activation of both proinflammatory and pro-resolving processes following nerve injury.

CX3CL1 overexpression markedly normalized CCI-induced DEGs and restored signaling across key biological pathways. Comparison of injured sciatic nerve transcriptomes from WT and CX3CL1-Tg mice identified 3,181 DEGs (FDR < 0.05, $|\log_2$ fold change$| > 1$), of which 1,442 (43.7%) were upregulated, and 1,706 (56.3%) were downregulated following CCI (**Fig. 6B, D**). Gene Ontology analysis revealed that CX3CL1 overexpression almost completely reversed the CCI-induced upregulation of immune-related biological processes and partially restored the downregulated pathways associated with synaptic transmission, synaptic organization, axonal outgrowth, and neuronal function (**Fig. 6G**).

CX3CL1 overexpression completely reversed the CCI-induced upregulation of key upstream cytokines identified in WT mice by Ingenuity Pathway Analysis (**Fig. 6H**). The majority of CCI-induced DEGs (2,854 genes) overlapped between WT and CX3CL1-Tg mice (**Fig. 6B, D**), confirming their specificity to nerve injury. Importantly, CX3CL1 overexpression markedly counteracted the inflammatory programs activated by CCI in WT mice. These included: (1) normalization of major inflammatory signaling pathways, such as TNF-α–NF-κB, IL-6–JAK–STAT3, PI3K–AKT–mTOR, and IFN-γ/IFN-α responses, as demonstrated by Gene Set Enrichment Analysis (GSEA) (**Fig. 7A**); (2) suppression of transcriptional upregulation of

proinflammatory chemokines and receptors, including members of the CCL/CCR and CXC/XCR families, as well as key upstream cytokines (TNF-α, IL-1β, IL-6, IL-18, IFN-γ) and their corresponding immune cell receptors (**Fig. 7B; Fig. S3, https://links.lww.com/ALN/E655**); and (3) normalization of transcripts associated with innate immune activation, including TREM (Triggering Receptors Expressed on Myeloid Cells)1–3, complement component C1q, S100a8, S100a9, inducible nitric oxide synthase (iNOS), arginase-1 (Arg1), the purinergic receptor P2X4, and toll-like receptors such as TLR4 (**Fig. S3, https://links.lww.com/ALN/E655**). In parallel with suppression of proinflammatory mediators, CX3CL1-Tg mice exhibited significant enhancement of TGF-β, Wnt/β-catenin, and Notch signaling (**Fig. S4, https://links.lww.com/ALN/E655**), as well as pathways involved in fatty acid metabolism (particularly β-oxidation), adipogenesis, and Hedgehog signaling, as revealed by GSEA (**Fig. 7A**). These pathways are known to promote polarization of proinflammatory M1 macrophages toward an anti-inflammatory M2 phenotype and to facilitate inflammation resolution and tissue repair. Consistent with these findings, CX3CL1-Tg mice displayed only modest activation of innate immune responses and no significant microglial activation in the spinal cord or brain, as assessed by fluorescence-activated cell sorting (FACS) analysis (**Fig. S5, https://links.lww.com/ALN/E655**).

DISCUSSION

This study provides a mechanistically integrated analysis of CX3CL1-mediated neuroimmune regulation in NP. Our findings demonstrate that enhancement of neuronal CX3CL1 signaling suppresses neuroinflammation and NP. These effects are mediated through two complementary and functionally distinct pathways: a CX3CR1-dependent pathway initiated by the CX3CL1 N-terminus that directly constrains immune cell activation, and a CX3CR1-

independent pathway mediated by the membrane-bound CX3CL1 C-terminus that promotes TGF-β family signaling within neurons. Together, these pathways restore neuroimmune homeostasis following nerve injury and define CX3CL1 as a critical molecular integrator of neuroinflammatory and neuroprotective processes (**Fig. 8**).

Following CCI, we observed rapid and sustained activation of microglia in the spinal cord and macrophages/monocytes in the DRG and sciatic nerve (**Fig. 1A-B**). This was accompanied by a marked reduction in CX3CL1-FL protein levels in the spinal cord (**Fig. 1C-F**), which reflects enhanced posttranslational processing rather than transcriptional repression as CX3CL1 transcript levels remained unchanged (**Fig. S1, https://links.lww.com/ALN/E655**). Consistent with this interpretation, CCI induced robust upregulation of multiple proteolytic enzymes, including cathepsin S (Cat-s), ADAM10, ADAM17, and MMP9, all of which are known to cleave CX3CL1-FL (**Fig. S2, https://links.lww.com/ALN/E655**).[28-30] This cleavage generates two biologically active products: a soluble N-terminus that signals through CX3CR1 on immune cells[28,29,31,32] and a membrane-retained C-terminus capable of initiating intracellular signaling within neurons.[25]

This injury-induced shift toward accelerated CX3CL1 processing has important functional consequences. The CX3CL1 N-terminus/CX3CR1 signaling restrains microglial and macrophage activation, thereby limiting production of proinflammatory cytokines.[33,34] In parallel, the C-terminus promotes transcription of TGF-β family genes and activates TGF-β/Smad2/3 signaling pathways within neurons.[21,25] In the present study, TGF-β1 protein expression closely paralleled changes in CX3CL1-FL and CX3CL1 C-terminus following CCI (**Fig. 1C-D, Fig. 5E-F**), supporting a mechanistic link between CX3CL1 processing and activation of neuroprotective TGF-β signaling.[21] Together, these findings suggest that nerve

injury disrupts the CX3CL1-mediated neuroimmune balance by accelerating its cleavage and altering the relative engagement of its downstream signaling pathways.

Neuron-specific augmentation of CX3CL1 signaling profoundly suppressed neuroinflammation and NP. CX3CL1 overexpression markedly suppressed microglial activation in the spinal cord (**Fig. 3**), reduced transcription of key proinflammatory cytokines (**Fig. 4**), and alleviated NP (**Fig. 5**). The molecular and cellular changes were accompanied by enhanced activation of TGF-β/Smad2/3 signaling and sustained elevation of TGF-β family proteins, particularly in the DRG and sciatic nerve (**Fig. 3C-E**). The close temporal and spatial correspondence between CX3CL1 overexpression, suppression of neuroinflammation, and analgesia effects strongly supports a causal role for CX3CL1 signaling in limiting NP. These findings align with accumulating evidence that CX3CL1/CX3CR1 signaling maintains microglia in a homeostatic state and restrains excessive neuroimmune activation.[35-42] However, they stand in contrast to a prevailing view that CX3CL1 signaling is intrinsically proinflammatory and pronociceptive.[5,6] Much of this earlier work relied on acute intrathecal administration of CX3CL1 or pharmacologic blockade of CX3CR1 approaches that do not distinguish between the distinct dual CX3CL1 signaling pathways. Notably, studies showing that inhibition of spinal microglial Cat-S reverses NP[43,44] suggest that Cat-S–CX3CL1 signaling is context-, compartment-, and fragment-dependent, and that CX3CL1 signaling is not a linear pathway. Cat-S inhibitors may reduce pain by blocking microglial Cat-S–mediated cleavage of CX3CL1, thereby preventing excessive release of pro-nociceptive soluble CX3CL1 that sustains microglial activation and cytokine production.[5,6,43] By contrast, neuronal CX3CL1 overexpression enhances homeostatic CX3CL1/CX3CR1 signaling and C-terminus-driven TGF-β pathways, producing analgesia through anti-inflammatory and neuroprotective mechanisms. Thus, excessive, acute

soluble CX3CL1/CX3CR1 activation in reactive microglia promotes nociception, whereas tonic neuronal CX3CL1 signaling coupled to C-terminus–mediated TGF-β pathways suppresses neuroinflammation[21,25] and produces analgesia (**Fig. 5**). Failure to recognize this duality likely explains prior conflicting conclusions and the limited efficacy of CX3CL1/CX3CR1-targeted therapies.[6]

Consistent with this revised framework, genetic deletion of CX3CR1 markedly exacerbated neuroinflammation following CCI (**Fig. 2)**. CX3CR1 KO mice exhibited prolonged microglial activation in the spinal cord and enhanced macrophage/monocyte activation in the DRG and sciatic nerve. These changes were accompanied by the accumulation of CX3CL1-FL and increased expression of TGF-β family proteins, particularly on the ipsilateral side of injury. These findings suggest that CX3CR1 signaling facilitates efficient utilization and turnover of CX3CL1-FL, preventing dysregulated accumulation and maladaptive immune responses.[11,12] In the absence of CX3CR1, CX3CL1-FL accumulates but cannot effectively engage its immunoregulatory function, resulting in exaggerated and persistent neuroinflammation.[45]

The CX3CL1-Tg mouse model provides a powerful approach to dissect the functional consequences of enhanced neuronal CX3CL1 signaling. In this model, selective neuronal overexpression of CX3CL1 (~3-fold) suppressed microglial activation (**Fig. 3**), reduced transcription of TNF-α, IL-1β, and IL-6 (**Fig. 4**), and enhanced TGF-β/Smad2/3 signaling following CCI (**Fig. 3**). Interestingly, although CX3CL1-FL and TGF-β family proteins were significantly increased in the DRG and sciatic nerve, their levels were not elevated in the spinal cord (**Fig. 3C–E**), likely reflecting higher proteolytic activity and rapid CX3CL1-FL cleavage in the spinal cord. Suppression of proinflammatory cytokines is a key mechanism by which CX3CL1 signaling mitigates NP. TNF-α, IL-1β, and IL-6 are well-established drivers of central

and peripheral sensitization.[46,47] These cytokines potentiate excitatory synaptic transmission, reduce inhibitory signaling, and lower neuronal firing thresholds in the dorsal horn.[3,48-52] In WT and CX3CR1 KO mice, CCI triggered rapid, robust, and sustained increases in these cytokines in both spinal and peripheral tissues (**Fig. 4**). In contrast, CX3CL1 overexpression markedly attenuated these responses in both magnitude and duration, indicating that CX3CL1 signaling constrains neuroinflammation during both initiation and maintenance phases of NP.

Behaviorally, enhanced CX3CL1 signaling translated into significant attenuation of NP with dramatic improvement in mechanical allodynia and thermal hyperalgesia (**Fig. 5A–D**). This is observed in both male and female mice. The absence of sex dimorphism is notable, given increasing recognition of sex-specific mechanisms in chronic pain. Microglial signaling has been proposed to predominate in males, while T cell–mediated mechanisms in females.[53,54] The broad efficacy in this study likely reflects the central role of CX3CL1 in coordinating interactions among neurons, microglia, and immune cells in both central and peripheral compartments.

Transcriptomic analyses provided further mechanistic insight into the global effects of CX3CL1 signaling. In WT mice, CCI induced extensive transcriptional reprogramming, with over 5,800 DEGs. More than half of these DEGs were upregulated and enriched in immune-related biological processes, including cytokine signaling, chemokine activity, and innate immune activation through intracellular inflammatory pathways such as PI3K–AKT, MAPK, and NF-κB signaling. In parallel, a substantial fraction of DEGs were downregulated and enriched in neuronal and synaptic processes, including synaptic transmission, axonal growth, and neuronal differentiation. This coordinated activation of immune programs and suppression of neuronal function is a hallmark of NP.[55-58] In CX3CL1-Tg mice, the magnitude of this transcriptional response was markedly reduced (**Fig. 6**). The total number of DEGs following

CCI was nearly halved, and many immune-related pathways were normalized. Enhanced CX3CL1 signaling corrected transcription of key cytokines and chemokines and restored expression of numerous receptors involved in immune activation, including members of the CCL/CCR and CXC/XCR families. Moreover, CX3CL1 overexpression counteracted activation of major inflammatory pathways, including NF-κB, IL-6–JAK–STAT3, PI3K–AKT–mTOR, and interferon signaling.

CX3CL1 signaling also broadly suppressed expression of innate immune amplifiers implicated in NP pathogenesis, including triggering receptors on myeloid cells (TREM1, TREM2, and TREM3), complement component C1q, calprotectin subunits S100A8 and S100A9, inducible nitric oxide synthase, purinergic receptor P2X4, and toll-like receptors such as TLR4. These molecules amplify inflammatory signaling and contribute to sustained immune activation and neuronal sensitization.[59-70] Their coordinated downregulation in CX3CL1-Tg mice underscores the capacity of CX3CL1 signaling to exert systems-level control over neuroimmune activation. In parallel, CX3CL1 overexpression enhanced transcription of genes involved in TGF-β, Wnt/β-catenin, and Notch signaling, as well as pathways regulating fatty acid metabolism and oxidative phosphorylation. These changes are consistent with metabolic reprogramming of macrophages toward anti-inflammatory, tissue-reparative phenotypes. Increased fatty acid oxidation and oxidative phosphorylation promote the transition from proinflammatory M1-like states to anti-inflammatory M2-like states, facilitating resolution of inflammation and tissue repair.[71]

Several limitations warrant consideration. While our data strongly implicates TGF-β/Smad signaling as a downstream effector of CX3CL1 C-terminal processing, direct manipulation of this pathway will be required to definitively establish causality. Future studies

incorporating selective CX3CR1 antagonists and TGF-β pathway inhibitors will be necessary to delineate the relative contributions of these pathways to the effects of CX3CL1 overexpression. In addition, the floor effects inherent to mechanical and thermal assays make it impractical to compare CX3CR1 KO mice with WT mice to detect more pain severity in CX3CR1 KO mice. Furthermore, the use of bulk real-time PCR of the spinal cord, DRG, and sciatic nerve and bulk RNA sequencing of the sciatic nerve is highly sensitive and robust for pathway-level changes with strong statistical power but is insufficient to dissect molecularly distinct neuronal and non-neuronal subtypes. Moreover, our findings pertain primarily to stimulus-evoked hypersensitivity. Future studies incorporating assays of spontaneous pain (e.g., home-cage behavior, conditioned place preference/aversion, or grimace scales) will be important to more comprehensively define the role of CX3CL1 overexpression in pain resolution. Finally, although our findings highlight substantial translational potential, further work will be required to determine whether selective modulation of CX3CL1 signaling domains can be safely and effectively leveraged in clinical settings.

Collectively, these findings support a dual-pathway framework in which CX3CL1 orchestrates neuroimmune interactions following nerve injury.[4] Injury-induced release of danger signals such as ATP,[72] α-synuclein,[73] and heat shock proteins[74] activate microglia and macrophages via purinergic[65,75] and toll-like receptors,[76-78] triggering inflammatory cascades that sensitize neurons and sustain pain.[79] CX3CL1 signaling counterbalances these processes through two synergistic mechanisms: suppression of immune cell activation via CX3CR1-dependent signaling and promotion of TGF-β–mediated neuroprotection and repair via C-terminal intracellular signaling. The coordinated engagement of these pathways dampens neuroinflammation, restores neuronal homeostasis, and accelerates the resolution of NP. This

study identifies CX3CL1 as a key regulator of neuroimmune homeostasis, challenges prevailing paradigms regarding its role in pain, and suggests that therapeutic strategies selectively targeting the protective components of CX3CL1 signaling may provide a novel and effective approach for NP management.

AUTHOR CONTRIBUTIONS:

Conceptualization: JC, QF

Methodology: QF, JZ, YK, QZ, YH, JL, FL, YY, MMH, RY, JC

Investigation: QF, JZ, YK, QZ, YH, JL, FL, YY, RY, JC

Statistical Analyses: QF, KS, JZ, MMH, YK, JC.

Visualization: KS, QF, JZ, YK, QZ, JL, FL, RY, JC

Funding acquisition: JC

Project administration: QF, JC

Supervision: JC

Writing – original draft: QF, JC

Writing – review & editing: JC

Acknowledgments: The authors are grateful to Drs. LiPing Liu, MD, Ph.D., for her substantial contributions to the early part of this work. The work is supported by the following grants:

National Institutes of Health NIH/NINDS/1UG3NS127258-01A1 UG3/UH3 (JC)

Department of Defense W81XWH-11-1-0672.10669042 (JC)

Lisa Dean Moseley Foundation (LDMF 0920JC, 1909JC, 1812JC, and 1709JC)

Cleveland Clinic Pain Management Innovations Fund #T56629 (JC).

Data and materials availability: All data are available in the main text and the supplementary materials (**https://links.lww.com/ALN/E655**). Raw data will be available with MTAs per Cleveland Clinic policies.

References

1. Colloca L, Ludman T, Bouhassira D, Baron R, Dickenson AH, Yarnitsky D, Freeman R, Truini A, Attal N, Finnerup NB, Eccleston C, Kalso E, Bennett DL, Dworkin RH, Raja SN: Neuropathic pain. Nat Rev Dis Primers 2017; 3: 17002

2. Cheng J: Is It Time to Redefine Neuropathic Pain? Pain Med 2021; 22: 2801-2802

3. Sommer C, Leinders M, Uceyler N: Inflammation in the pathophysiology of neuropathic pain. Pain 2018; 159: 595-602

4. Buchheit T, Huh Y, Maixner W, Cheng J, Ji RR: Neuroimmune modulation of pain and regenerative pain medicine. J Clin Invest 2020; 130: 2164-2176

5. Clark AK, Malcangio M: Fractalkine/CX3CR1 signaling during neuropathic pain. Front Cell Neurosci 2014; 8: 121

6. Silva R, Malcangio M: Fractalkine/CX3CR1 Pathway in Neuropathic Pain: An Update. Front. Pain Res 2021

7. Nimmerjahn A, Kirchhoff F, Helmchen F: Resting microglial cells are highly dynamic surveillants of brain parenchyma in vivo. Science 2005; 308: 1314-8

8. Ji RR, Berta T, Nedergaard M: Glia and pain: is chronic pain a gliopathy? Pain 2013; 154 Suppl 1: S10-s28

9. Bazan JF, Bacon KB, Hardiman G, Wang W, Soo K, Rossi D, Greaves DR, Zlotnik A, Schall TJ: A new class of membrane-bound chemokine with a CX3C motif. Nature 1997; 385: 640-4

10. Pan Y, Lloyd C, Zhou H, Dolich S, Deeds J, Gonzalo JA, Vath J, Gosselin M, Ma J, Dussault B, Woolf E, Alperin G, Culpepper J, Gutierrez-Ramos JC, Gearing D: Neurotactin, a membrane-anchored chemokine upregulated in brain inflammation. Nature 1997; 387: 611-7

11. Slusarczyk J, Trojan E, Glombik K, Chamera K, Roman A, Budziszewska B, Basta-Kaim A: Fractalkine Attenuates Microglial Cell Activation Induced by Prenatal Stress. Neural Plast 2016; 2016: 7258201

12. Ransohoff RM, El Khoury J: Microglia in Health and Disease. Cold Spring Harb Perspect Biol 2015; 8: a020560

13. Imai T, Hieshima K, Haskell C, Baba M, Nagira M, Nishimura M, Kakizaki M, Takagi S, Nomiyama H, Schall TJ, Yoshie O: Identification and molecular characterization of fractalkine receptor CX3CR1, which mediates both leukocyte migration and adhesion. Cell 1997; 91: 521-30

14. Lauro C, Catalano M, Trettel F, Limatola C: Fractalkine in the nervous system: neuroprotective or neurotoxic molecule? Ann N Y Acad Sci 2015; 1351: 141-8

15. Souza GR, Talbot J, Lotufo CM, Cunha FQ, Cunha TM, Ferreira SH: Fractalkine mediates inflammatory pain through activation of satellite glial cells. Proc Natl Acad Sci U S A 2013; 110: 11193-8

16. Staniland AA, Clark AK, Wodarski R, Sasso O, Maione F, D'Acquisto F, Malcangio M: Reduced inflammatory and neuropathic pain and decreased spinal microglial response in fractalkine receptor (CX3CR1) knockout mice. J Neurochem 2010; 114: 1143-57

17. Holmes FE, Arnott N, Vanderplank P, Kerr NC, Longbrake EE, Popovich PG, Imai T, Combadiere C, Murphy PM, Wynick D: Intra-neural administration of fractalkine attenuates neuropathic pain-related behaviour. J Neurochem 2008; 106: 640-9

18. Liu C, Hong K, Chen H, Niu Y, Duan W, Liu Y, Ji Y, Deng B, Li Y, Li Z, Wen D, Li C: Evidence for a protective role of the CX3CL1/CX3CR1 axis in a model of amyotrophic lateral sclerosis. Biol Chem 2019; 400: 651-661

19. Finneran DJ, Nash KR: Neuroinflammation and fractalkine signaling in Alzheimer's disease. J Neuroinflammation 2019; 16: 30

20. Subbarayan MS, Joly-Amado A, Bickford PC, Nash KR: CX3CL1/CX3CR1 signaling targets for the treatment of neurodegenerative diseases. Pharmacol Ther 2022; 231: 107989

21. Fan Q, He W, Gayen M, Benoit MR, Luo X, Hu X, Yan R: Activated CX3CL1/Smad2 Signals Prevent Neuronal Loss and Alzheimer's Tau Pathology-Mediated Cognitive Dysfunction. J Neurosci 2020; 40: 1133-1144

22. Shen J, Fox LE, Cheng J: Differential effects of peripheral versus central coadministration of qx-314 and capsaicin on neuropathic pain in rats. Anesthesiology 2012; 117: 365-380

23. Jung S, Aliberti J, Graemmel P, Sunshine MJ, Kreutzberg GW, Sher A, Littman DR: Analysis of fractalkine receptor CX(3)CR1 function by targeted deletion and green fluorescent protein reporter gene insertion. Mol Cell Biol 2000; 20: 4106-14

24. Yamasaki R, Lu H, Butovsky O, Ohno N, Rietsch AM, Cialic R, Wu PM, Doykan CE, Lin J, Cotleur AC, Kidd G, Zorlu MM, Sun N, Hu W, Liu L, Lee JC, Taylor SE, Uehlein L, Dixon D, Gu J, Floruta CM, Zhu M, Charo IF, Weiner HL, Ransohoff RM: Differential roles of microglia and monocytes in the inflamed central nervous system. J Exp Med 2014; 211: 1533-49

25. Fan Q, Gayen M, Singh N, Gao F, He W, Hu X, Tsai LH, Yan R: The intracellular domain of CX3CL1 regulates adult neurogenesis and Alzheimer's amyloid pathology. J Exp Med 2019; 216: 1891-1903

26. Ge Y, Xu W, Chen Z, Zhang H, Zhang W, Chen J, Huang J, Du W, Tong P, Shan L, Zhou L: Nanofat lysate ameliorates pain and cartilage degradation of osteoarthritis through activation of TGF-β-Smad2/3 signaling of chondrocytes. Front Pharmacol 2023; 14: 900205

27. Gayen M, Benoit MR, Fan Q, Hudobenko J, Yan R: The CX3CL1 intracellular domain exhibits neuroprotection via insulin receptor/insulin-like growth factor receptor signaling. J Biol Chem 2022; 298: 102532

28. Hundhausen C, Misztela D, Berkhout TA, Broadway N, Saftig P, Reiss K, Hartmann D, Fahrenholz F, Postina R, Matthews V, Kallen KJ, Rose-John S, Ludwig A: The disintegrin-like metalloproteinase ADAM10 is involved in constitutive cleavage of CX3CL1 (fractalkine) and regulates CX3CL1-mediated cell-cell adhesion. Blood 2003; 102: 1186-95

29. Garton KJ, Gough PJ, Blobel CP, Murphy G, Greaves DR, Dempsey PJ, Raines EW: Tumor necrosis factor-alpha-converting enzyme (ADAM17) mediates the cleavage and shedding of fractalkine (CX3CL1). J Biol Chem 2001; 276: 37993-8001

30. Cook A, Hippensteel R, Shimizu S, Nicolai J, Fatatis A, Meucci O: Interactions between chemokines: regulation of fractalkine/CX3CL1 homeostasis by SDF/CXCL12 in cortical neurons. J Biol Chem 2010; 285: 10563-71

31. Gunner G, Cheadle L, Johnson KM, Ayata P, Badimon A, Mondo E, Nagy MA, Liu L, Bemiller SM, Kim KW, Lira SA, Lamb BT, Tapper AR, Ransohoff RM, Greenberg ME, Schaefer A, Schafer DP: Sensory lesioning induces microglial synapse elimination via ADAM10 and fractalkine signaling. Nat Neurosci 2019; 22: 1075-1088

32. Chapman GA, Moores K, Harrison D, Campbell CA, Stewart BR, Strijbos PJ: Fractalkine cleavage from neuronal membranes represents an acute event in the inflammatory response to excitotoxic brain damage. J Neurosci 2000; 20: Rc87

33. Liu H, Jiang D: Fractalkine/CX3CR1 and atherosclerosis. Clin Chim Acta 2011; 412: 1180-6

34. Winter AN, Subbarayan MS, Grimmig B, Weesner JA, Moss L, Peters M, Weeber E, Nash K, Bickford PC: Two forms of CX3CL1 display differential activity and rescue cognitive deficits in CX3CL1 knockout mice. J Neuroinflammation 2020; 17: 157

35. Soriano SG, Amaravadi LS, Wang YF, Zhou H, Yu GX, Tonra JR, Fairchild-Huntress V, Fang Q, Dunmore JH, Huszar D, Pan Y: Mice deficient in fractalkine are less susceptible to cerebral ischemia-reperfusion injury. J Neuroimmunol 2002; 125: 59-65

36. Cardona AE, Pioro EP, Sasse ME, Kostenko V, Cardona SM, Dijkstra IM, Huang D, Kidd G, Dombrowski S, Dutta R, Lee JC, Cook DN, Jung S, Lira SA, Littman DR, Ransohoff RM: Control of microglial neurotoxicity by the fractalkine receptor. Nat Neurosci 2006; 9: 917-24

37. Huang D, Shi FD, Jung S, Pien GC, Wang J, Salazar-Mather TP, He TT, Weaver JT, Ljunggren HG, Biron CA, Littman DR, Ransohoff RM: The neuronal chemokine CX3CL1/fractalkine selectively recruits NK cells that modify experimental autoimmune encephalomyelitis within the central nervous system. Faseb j 2006; 20: 896-905

38. Denes A, Vidyasagar R, Feng J, Narvainen J, McColl BW, Kauppinen RA, Allan SM: Proliferating resident microglia after focal cerebral ischaemia in mice. J Cereb Blood Flow Metab 2007; 27: 1941-53

39. Cipriani R, Villa P, Chece G, Lauro C, Paladini A, Micotti E, Perego C, De Simoni MG, Fredholm BB, Eusebi F, Limatola C: CX3CL1 is neuroprotective in permanent focal cerebral ischemia in rodents. J Neurosci 2011; 31: 16327-35

40. Lee S, Xu G, Jay TR, Bhatta S, Kim KW, Jung S, Landreth GE, Ransohoff RM, Lamb BT: Opposing effects of membrane-anchored CX3CL1 on amyloid and tau pathologies via the p38 MAPK pathway. J Neurosci 2014; 34: 12538-46

41. Bachstetter AD, Morganti JM, Jernberg J, Schlunk A, Mitchell SH, Brewster KW, Hudson CE, Cole MJ, Harrison JK, Bickford PC, Gemma C: Fractalkine and CX 3 CR1 regulate hippocampal neurogenesis in adult and aged rats. Neurobiol Aging 2011; 32: 2030-44

42. Sheridan GK, Murphy KJ: Neuron-glia crosstalk in health and disease: fractalkine and CX3CR1 take centre stage. Open Biol 2013; 3: 130181

43. Clark AK, Yip PK, Grist J, Gentry C, Staniland AA, Marchand F, Dehvari M, Wotherspoon G, Winter J, Ullah J, Bevan S, Malcangio M: Inhibition of spinal microglial cathepsin S for the reversal of neuropathic pain. Proc Natl Acad Sci U S A 2007; 104: 10655-60

44. Hewitt E, Pitcher T, Rizoska B, Tunblad K, Henderson I, Sahlberg BL, Grabowska U, Classon B, Edenius C, Malcangio M, Lindström E: Selective Cathepsin S Inhibition with MIV-247 Attenuates Mechanical Allodynia and Enhances the Antiallodynic Effects of Gabapentin and Pregabalin in a Mouse Model of Neuropathic Pain. J Pharmacol Exp Ther 2016; 358: 387-96

45. Castro-Sanchez S, Garcia-Yague AJ, Lopez-Royo T, Casarejos M, Lanciego JL, Lastres-Becker I: Cx3cr1-deficiency exacerbates alpha-synuclein-A53T induced neuroinflammation and neurodegeneration in a mouse model of Parkinson's disease. Glia 2018; 66: 1752-1762

46. Zhang JM, An J: Cytokines, inflammation, and pain. Int Anesthesiol Clin 2007; 45: 27-37

47. Basbaum AI, Bautista DM, Scherrer G, Julius D: Cellular and molecular mechanisms of pain. Cell 2009; 139: 267-84

48. Pinho-Ribeiro FA, Verri WA, Jr., Chiu IM: Nociceptor Sensory Neuron-Immune Interactions in Pain and Inflammation. Trends Immunol 2017; 38: 5-19

49. Malcangio M: Role of the immune system in neuropathic pain. Scand J Pain 2019; 20: 33-37

50. Ming Z, Criswell HE, Breese GR: Evidence for TNFα action on excitatory and inhibitory neurotransmission in the central amygdala: a brain site influenced by stress. Brain Behav Immun 2013; 33: 102-11

51. Olmos G, Lladó J: Tumor necrosis factor alpha: a link between neuroinflammation and excitotoxicity. Mediators Inflamm 2014; 2014: 861231

52. Pizzo PA, Clark NM: Alleviating suffering 101--pain relief in the United States. N Engl J Med 2012; 366: 197-9

53. Tansley S, Uttam S, Ureña Guzmán A, Yaqubi M, Pacis A, Parisien M, Deamond H, Wong C, Rabau O, Brown N, Haglund L, Ouellet J, Santaguida C, Ribeiro-da-Silva A, Tahmasebi S, Prager-Khoutorsky M, Ragoussis J, Zhang J, Salter MW, Diatchenko L, Healy LM, Mogil JS, Khoutorsky A: Single-cell RNA sequencing reveals time- and sex-specific responses of mouse spinal cord microglia to peripheral nerve injury and links ApoE to chronic pain. Nat Commun 2022; 13: 843

54. Sorge RE, Mapplebeck JC, Rosen S, Beggs S, Taves S, Alexander JK, Martin LJ, Austin JS, Sotocinal SG, Chen D, Yang M, Shi XQ, Huang H, Pillon NJ, Bilan PJ, Tu Y, Klip A, Ji RR, Zhang J, Salter MW, Mogil JS: Different immune cells mediate mechanical pain hypersensitivity in male and female mice. Nat Neurosci 2015; 18: 1081-3

55. Liu W, Lv Y, Ren F: PI3K/Akt Pathway is Required for Spinal Central Sensitization in Neuropathic Pain. Cell Mol Neurobiol 2018; 38: 747-755

56. Ji RR, Nackley A, Huh Y, Terrando N, Maixner W: Neuroinflammation and Central Sensitization in Chronic and Widespread Pain. Anesthesiology 2018; 129: 343-366

57. Ji RR, Suter MR: p38 MAPK, microglial signaling, and neuropathic pain. Mol Pain 2007; 3: 33

58. Dominguez E, Rivat C, Pommier B, Mauborgne A, Pohl M: JAK/STAT3 pathway is activated in spinal cord microglia after peripheral nerve injury and contributes to neuropathic pain development in rat. J Neurochem 2008; 107: 50-60

59. Gebhardt C, Riehl A, Durchdewald M, Németh J, Fürstenberger G, Müller-Decker K, Enk A, Arnold B, Bierhaus A, Nawroth PP, Hess J, Angel P: RAGE signaling sustains inflammation and promotes tumor development. J Exp Med 2008; 205: 275-85

60. van Lent PL, Hofkens W, Blom AB, Grevers L, Sloetjes A, Takahashi N, van Tits LJ, Vogl T, Roth J, de Winther MP, van den Berg WB: Scavenger receptor class A type I/II determines matrix metalloproteinase-mediated cartilage destruction and chondrocyte death in antigen-induced arthritis. Arthritis Rheum 2009; 60: 2954-65

61. Hobbs JA, May R, Tanousis K, McNeill E, Mathies M, Gebhardt C, Henderson R, Robinson MJ, Hogg N: Myeloid cell function in MRP-14 (S100A9) null mice. Mol Cell Biol 2003; 23: 2564-76

62. Leukert N, Vogl T, Strupat K, Reichelt R, Sorg C, Roth J: Calcium-dependent tetramer formation of S100A8 and S100A9 is essential for biological activity. J Mol Biol 2006; 359: 961-72

63. Nakatsuji T, Gallo RL: Antimicrobial peptides: old molecules with new ideas. J Invest Dermatol 2012; 132: 887-95

64. Inoue K: Role of the P2X4 receptor in neuropathic pain. Curr Opin Pharmacol 2019; 47: 33-39

65. Inoue K, Tsuda M: Microglia in neuropathic pain: cellular and molecular mechanisms and therapeutic potential. Nat Rev Neurosci 2018; 19: 138-152

66. Liu X, Yang W, Zhu C, Sun S, Wu S, Wang L, Wang Y, Ge Z: Toll-like receptors and their role in neuropathic pain and migraine. Mol Brain 2022; 15: 73

67. Harima A, Shimizu H, Takagi H: Analgesic effect of L-arginine in patients with persistent pain. Eur Neuropsychopharmacol 1991; 1: 529-33

68. Rocha PA, Ferreira AFB, Da Silva JT, Alves AS, Martins DO, Britto LRG, Chacur M: Effects of selective inhibition of nNOS and iNOS on neuropathic pain in rats. Mol Cell Neurosci 2020; 105: 103497

69. Kishore U, Reid KB: C1q: structure, function, and receptors. Immunopharmacology 2000; 49: 159-70

70. Zhang C, Kan X, Zhang B, Ni H, Shao J: The role of triggering receptor expressed on myeloid cells-1 (TREM-1) in central nervous system diseases. Mol Brain 2022; 15: 84

71. Batista-Gonzalez A, Vidal R, Criollo A, Carreño LJ: New Insights on the Role of Lipid Metabolism in the Metabolic Reprogramming of Macrophages. Front Immunol 2019; 10: 2993

72. Muñoz MF, Griffith TN, Contreras JE: Mechanisms of ATP release in pain: role of pannexin and connexin channels. Purinergic Signal 2021; 17: 549-561

73. Ferreira N, Gonçalves NP, Jan A, Jensen NM, van der Laan A, Mohseni S, Vægter CB, Jensen PH: Trans-synaptic spreading of alpha-synuclein pathology through sensory afferents leads to sensory nerve degeneration and neuropathic pain. Acta Neuropathol Commun 2021; 9: 31

74. Klass MG, Gavrikov V, Krishnamoorthy M, Csete M: Heat shock proteins, endothelin, and peripheral neuronal injury. Neurosci Lett 2008; 433: 188-93

75. Kohno K, Tsuda M: Role of microglia and P2X4 receptors in chronic pain. Pain Rep 2021; 6: e864

76. Kim D, Kim MA, Cho IH, Kim MS, Lee S, Jo EK, Choi SY, Park K, Kim JS, Akira S, Na HS, Oh SB, Lee SJ: A critical role of toll-like receptor 2 in nerve injury-induced spinal cord glial cell activation and pain hypersensitivity. J Biol Chem 2007; 282: 14975-83

77. Obata K, Katsura H, Miyoshi K, Kondo T, Yamanaka H, Kobayashi K, Dai Y, Fukuoka T, Akira S, Noguchi K: Toll-like receptor 3 contributes to spinal glial activation and tactile allodynia after nerve injury. J Neurochem 2008; 105: 2249-59

78. Ribeiro P, Castro MV, Perez M, Cartarozzi LP, Spejo AB, Chiarotto GB, Augusto TM, Oliveira ALR: Toll-like receptor 4 (TLR4) influences the glial reaction in the spinal cord and the neural response to injury following peripheral nerve crush. Brain Res Bull 2020; 155: 67-80

79. Calvo M, Bennett DL: The mechanisms of microgliosis and pain following peripheral nerve injury. Exp Neurol 2012; 234: 271-82

Figure Legends

Figure 1. Chronic constriction injury activates CX3CR1-positive cells and reduces full-length CX3CL1 and TGF-β family proteins.

A-B. Confocal microscopy (A) and quantitative data (B) demonstrate a time-dependent increase in CX3CR1 expression in the sciatic nerve (SN), dorsal root ganglia (DRG), and spinal cord (SC) following chronic constriction injury (CCI) of the sciatic nerve (scale bar = 30 μm). Measurements shown in Fig.1B were obtained from independent groups of mice at each time point; therefore, statistical comparisons were performed using one-way ANOVA.

C–D. Western blot protein expression of full-length CX3CL1 (CX3CL1-FL) and TGF-β family members in the spinal cord is reduced after CCI, with the greatest decrease observed between days 7 and 14 post-injury (C). Quantitative analysis from 3 independent experiments (N=3) (D) shows parallel reductions in CX3CL1-FL and TGF-β family protein levels. Data are presented as mean ± SD. * $P < 0.05$, ** $P < 0.01$ (one-way ANOVA with Tukey post hoc test).

E–F. Western blot analysis reveals reduced CX3CL1-FL and TGF-β family protein expression on the ipsilateral side of the DRG and SN, and bilaterally in the SC, on day 7 post-CCI (**E**). The lower CX3CL1-FL signal in DRG and SN reflects limited tissue availability. Quantification (**F**) confirms decreased CX3CL1-FL protein levels normalized to β-actin.

Data are presented as mean ± SD from 4 independent experiments (N=4). * $P < 0.05$, ** $P < 0.01$, ***$P < 0.001$, ****$P < 0.0001$ (one-way ANOVA with Tukey post hoc test). Ipsi, ipsilateral; Contra, contralateral; Sham, sham control.

Figure 2. Disruption of CX3CL1/CX3CR1 signaling prolongs chronic constriction injury-induced microglial activation, leading to the accumulation of CX3CL1-FL and TGF-β family proteins.

A–B. Confocal microscopy (A) and quantitative analysis (B) demonstrate sustained activation of microglia ($CX3CR1^{+}$ cells) in both sides of the spinal cord at days 7 and 28 after chronic constriction injury (CCI) in $CX3CR1^{GFP/+}$ and $CX3CR1^{GFP/GFP}$ mice. The white arrow denotes the ipsilateral dorsal horn (scale bar = 30 μm). Quantitative fluorescence intensity data are from 4 independent experiments (N = 4). Data are presented as mean ± SD. * $P < 0.05$, ** $P < 0.01$, **** $P < 0.0001$ (one-way ANOVA with Tukey post hoc test). Ipsi, ipsilateral; Contra, contralateral; Sham, sham control.

C–D. Western blot analysis shows CX3CL1 full-length (CX3CL1-FL) protein expression in the spinal cord of wild-type, $CX3CR1^{GFP/+}$, and $CX3CR1^{GFP/GFP}$ mice (C), with corresponding quantification (D) of relative CX3CL1-FL levels normalized to β-actin (N = 4). Data are presented as mean ± SD. *** $P < 0.001$ (one-way ANOVA with Tukey post hoc test).

E–G. Expression of CX3CL1 and TGF-β family proteins in the spinal cord on both sides at day 7 after CCI in $CX3CR1^{GFP/+}$ and $CX3CR1^{GFP/GFP}$ mice (**E**). Quantitative analyses from 3 independent experiments (N = 3) show relative protein levels of CX3CL1 (**F**) and TGF-β family members (**G**), normalized to β-actin. Data are presented as mean ± SD.** $P < 0.01$, *** $P < 0.001$, **** $P < 0.0001$ (Two-way ANOVA).

Figure 3. CX3CL1 overexpression enhances TGF-β/Smad2/3 signaling and suppresses chronic constriction injury-induced microglial activation.

A–B. Microglial activation, assessed by green fluorescent protein (GFP) intensity, is significantly reduced in CX3CL1-overexpressing mice ($CX3CL1;CX3CR1^{GFP/+;}$ HA-tagged CX3CL1 detected with anti-HA antibody, red) compared with CX3CR1GFP/+ and CX3CR1GFP/GFP mice. Representative images of the dorsal horns (**A**, white arrows) and quantitative analysis (**B**) from 3 independent experiments (N = 3) are shown. Data are presented

as mean ± SD. * P < 0.05, ** P < 0.01, **** P < 0.0001 (one-way ANOVA with Tukey post hoc test). Ipsi, ipsilateral; Contra, contralateral; Sham, sham control.

C–E. Protein expression of CX3CL1 and TGF-β/Smad2/3 is increased in the sciatic nerve (**C**), dorsal root ganglia (**D**), and spinal cord (**E**) of CX3CL1-overexpressing mice compared with $CX3CR1^{GFP/+}$ controls at day 7 after chronic constriction injury. Quantitative data normalized to β-actin are from 4 independent experiments (N = 4). Data are presented as mean ± SD. * P < 0.05, ** P < 0.01, **** P < 0.0001 (one-way ANOVA with Tukey post hoc test). Ipsi, ipsilateral; Contra, contralateral; Sham, sham control.

Figure 4. CX3CL1 overexpression suppresses transcription of proinflammatory cytokines. Real-time PCR analysis demonstrates a significant and sustained reduction in gene expression of TNF-α, IL-1β, and IL-6 in the spinal cord (A) and sciatic nerve (B) at multiple time points following chronic constriction injury (CCI) in CX3CL1-Tg mice compared with CX3CR1GFP/GFP and wild-type controls. Time-course data and area under the curve analyses are shown. Data represent mean ± SD from 6 independent experiments (N = 6). Two-way ANOVA was applied to the time-course gene expression data to assess the effects of genotype and time; area under the curve (AUC) values are presented for descriptive purposes and visualization only, and no statistical comparisons were performed on AUC. Two-way ANOVA test with Bonferroni's correction for multiple comparisons: WT vs CX3CL1-Tg *P<0.05, ** P<0.01, *** P<0.001; CX3CL1-Tg vs. $CX3CR1^{GFP/GFP}$ $^{\#}$P<0.05, $^{\#\#}$P<0.01, $^{\#\#\#}$P<0.001**.**

Figure 5. CX3CL1 overexpression attenuates chronic constriction injury-induced mechanical and thermal hyperalgesia and increases TGF-β family protein expression in the sciatic nerve.

A–D. Mechanical allodynia and thermal hyperalgesia, assessed by paw withdrawal threshold (PWT) using von Frey testing and paw withdrawal latency (PWL) using Hargreaves testing, are significantly alleviated in CX3CL1-overexpressing (CX3CL1-Tg) mice compared with wild-type (WT) controls. The effects peak approximately two weeks after CCI and are evident in both male (A) and female (B) mice (n = 10 per group). When data from both sexes are combined, significant effects are already evident by day 3 post-CCI (C–D, n = 20). Data are mean ± SD. * P < 0.05, ** P < 0.01, ***P<0.001, **** P<0.0001 (repeated measures ANOVA).

E–F. In CX3CL1-Tg mice, full-length CX3CL1 (CX3CL1-FL) expression sharply decreases during the first two weeks post-CCI and gradually recovers thereafter. In contrast, CX3CL1 C-terminus levels significantly increase in a biphasic fashion, first peaking at post-CCI day 3 and second peaking at post-CCI day 21. TGF-β family protein expression rises markedly with a similar temporal pattern to CX3CL1 C-terminal. Quantitative data normalized to β-actin are from 4 independent experiments (N = 4). Data are presented as mean ± SD. * P < 0.05, ** P < 0.01, *** P < 0.001 (one-way ANOVA with Tukey post hoc test).

Figure 6. CX3CL1 overexpression reverses chronic constriction injury-induced transcriptional reprogramming.

A. Principal component analysis of RNA-seq libraries shows clear separation among experimental groups: CX3CL1-Tg control (Tg), CX3CL1-Tg–CCI (Tg-CCI), wild-type control (WT), and WT-CCI.

B. Venn diagram depicts shared and distinct differentially expressed genes (DEGs) associated with CCI in WT mice (WT-CCI vs WT) and CX3CL1-overexpressing mice (Tg-CCI vs WT-CCI).

C–D. Hierarchical clustering heatmaps of DEGs comparing WT control vs WT-CCI (C) and WT control vs CX3CL1-Tg–CCI (D); upregulated genes are shown in red and downregulated genes in blue.

E–F. Gene Ontology (GO) enrichment analysis identifies the top 25 biological processes associated with CCI-induced DEGs in WT mice (false discovery rate < 0.05; fold change > 2 or < 0.5) (top 10 processes are shown for clarity), with corresponding Ingenuity Pathway Analysis (IPA) showing activated (orange) and inhibited (blue) pathways.

G–H. GO and IPA analyses in CX3CL1-Tg mice reveal near-complete reversal of CCI-induced pathway activation, with signaling shifting from activation to inhibition relative to WT-CCI mice.

Figure 7. CX3CL1 overexpression suppresses chronic constriction injury-induced inflammatory signaling pathways.

A. Gene set enrichment analysis (GSEA) reveals significant overlap in DEG sets between WT-CCI and CX3CL1-Tg–CCI groups.

B. Schematic summary illustrating reversal of CCI-induced intracellular inflammatory signaling by CX3CL1 overexpression. In WT mice, CCI activates toll-like, purinergic, chemokine/cytokine, and T-cell receptors, leading to activation of TLR, PI3K–AKT, and RAS–RAF–MAPK (p38, ERK, JNK) pathways and downstream transcription factors NF-κB and AP-1, resulting in increased proinflammatory cytokine production. CX3CL1 overexpression inhibits receptor activation, intracellular signaling cascades, and transcriptional responses, thereby reducing inflammatory cytokine synthesis. Genes upregulated in WT-CCI relative to WT control are shown in red, and genes downregulated in CX3CL1-Tg–CCI relative to WT-CCI are shown in blue.

Figure 8. A dual-pathway model of CX3CL1-mediated neuroimmune regulation in the spinal cord in neuropathic pain.

Schematic illustration of CX3CL1 signaling neuroimmune framework following nerve injury. In wild-type mice, CCI triggers release of danger-associated signals from nociceptors, activating microglia and peripheral immune cells via purinergic, toll-like, and cytokine/chemokine receptors. This activation engages intracellular PI3K–AKT and RAS–RAF–MAPK signaling cascades, leading to NF-κB and AP-1–mediated transcription of proinflammatory cytokines and subsequent neuronal sensitization. CX3CL1 signaling operates through dual protective pathways: the soluble N-terminus suppresses microglial activation and cytokine production via CX3CR1, while the membrane-bound C-terminus promotes TGF-β/Smad2/3 and Hedgehog signaling to reduce neuronal hyperexcitability and enhance neural repair. Coordinated activation of these pathways attenuates central and peripheral sensitization, limits neuroinflammation, and promotes resolution of neuropathic pain.

Supplementary digital contents, https://links.lww.com/ALN/E655

S1. Basal cytokines & CCI-induced CX3CR1

S2. RNA-seq DEGs in WT vs CX3CL1-Tg

S3. Cytokine increase in CX3CR1 KO spinal cord

S4. Upregulated pathways in CX3CL1-Tg mice

S5. CX3CL1 overexpression & microglial activation

Figure 1

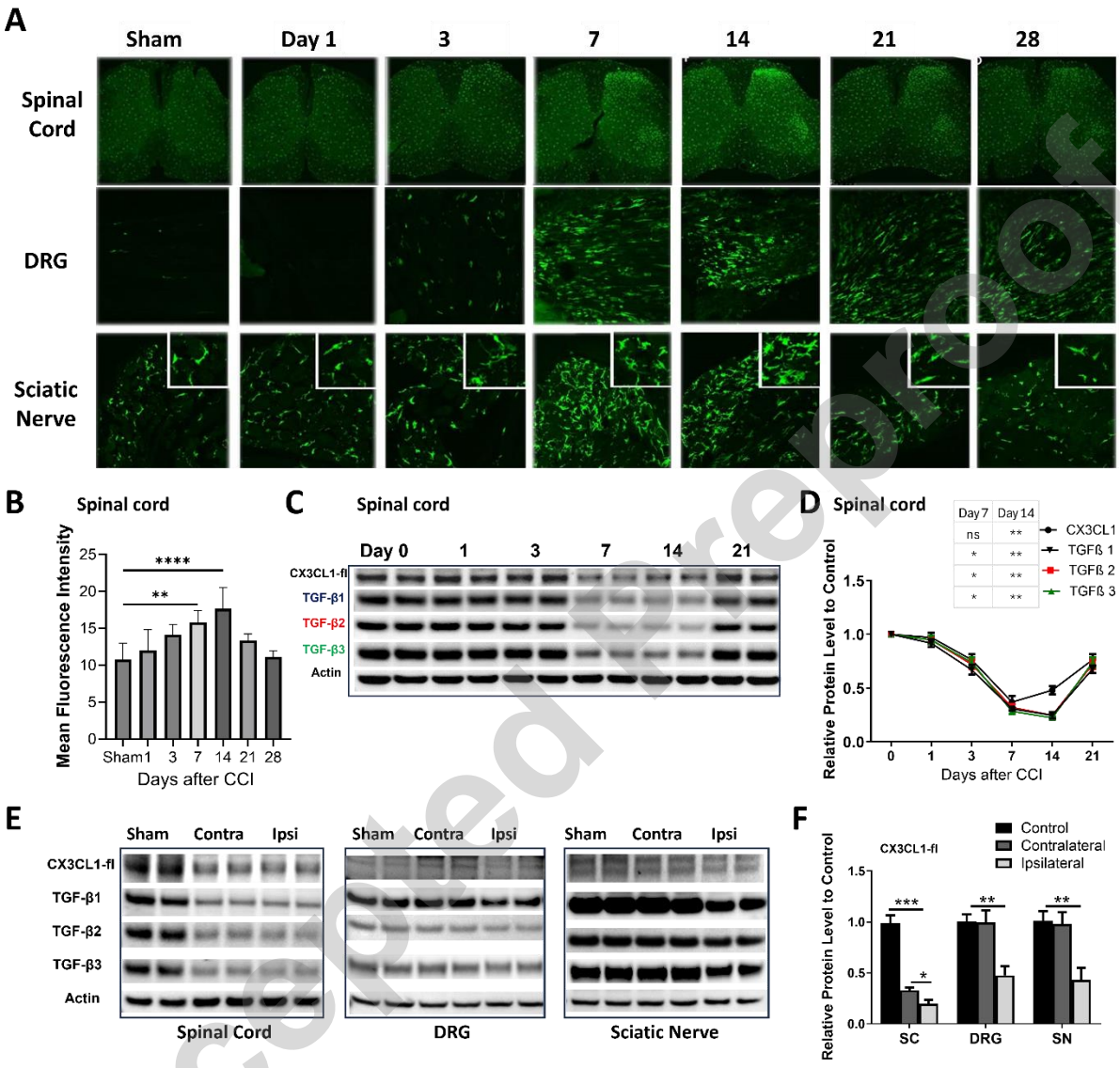

Figure 2

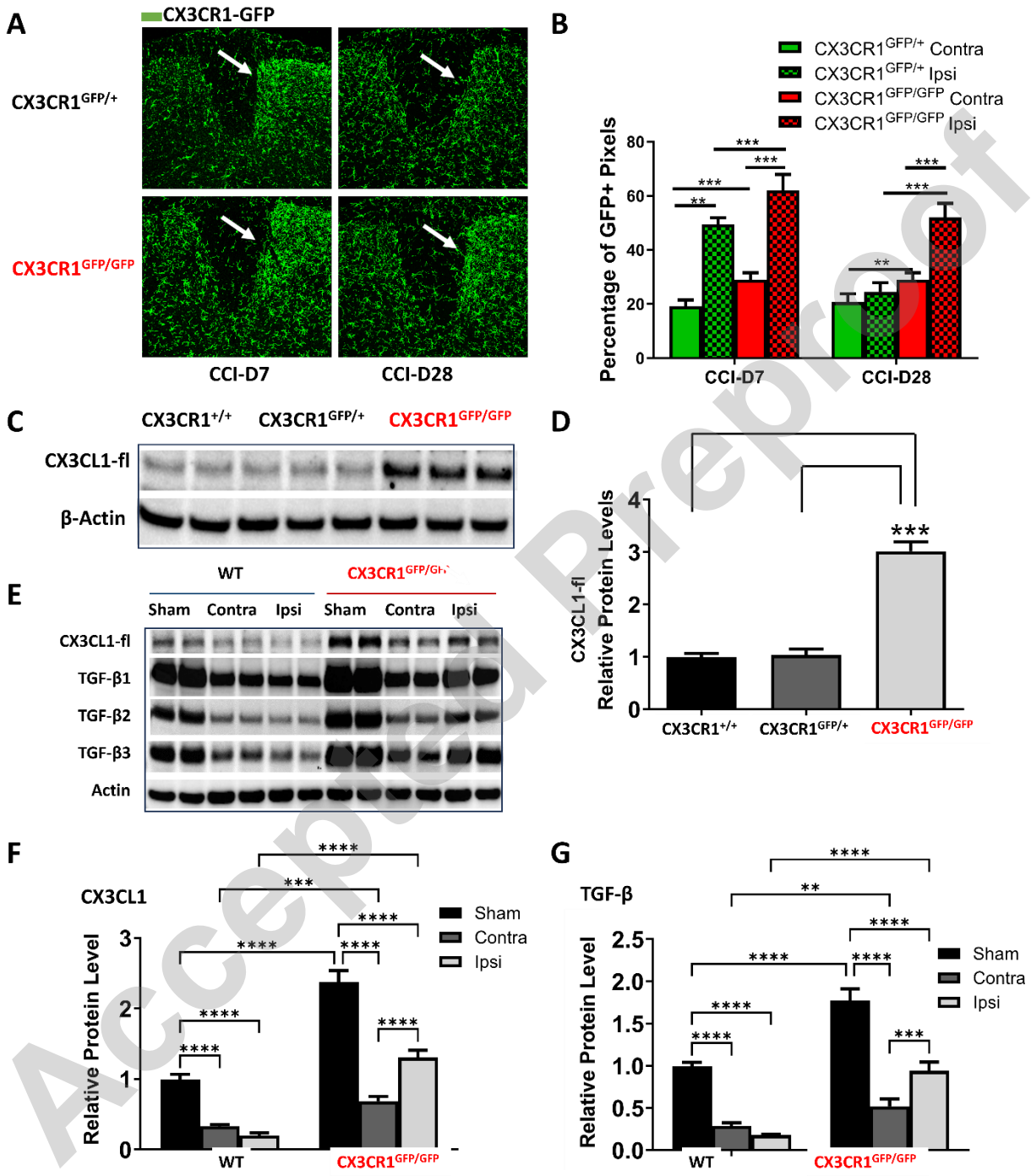

Figure 3

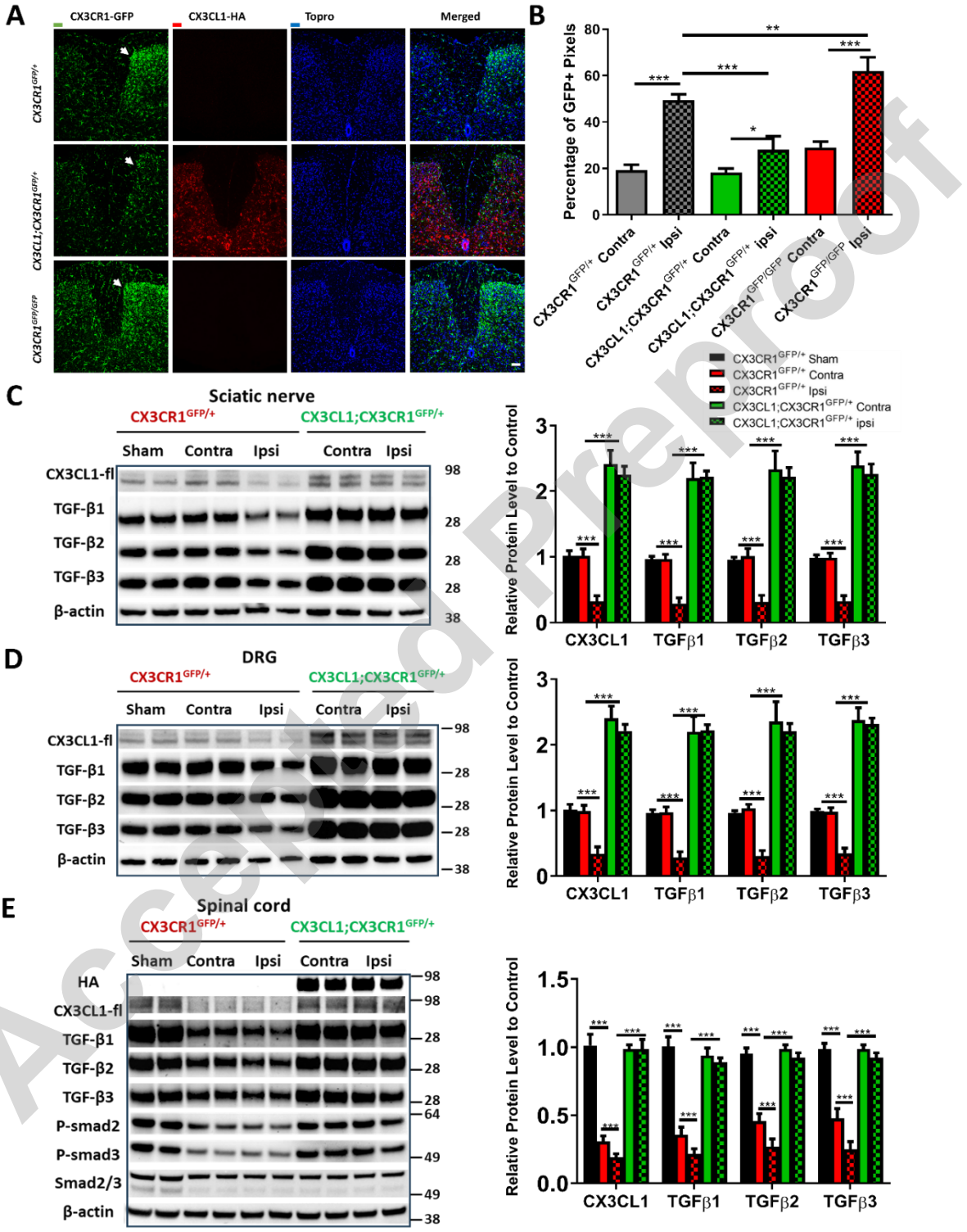

Figure 4

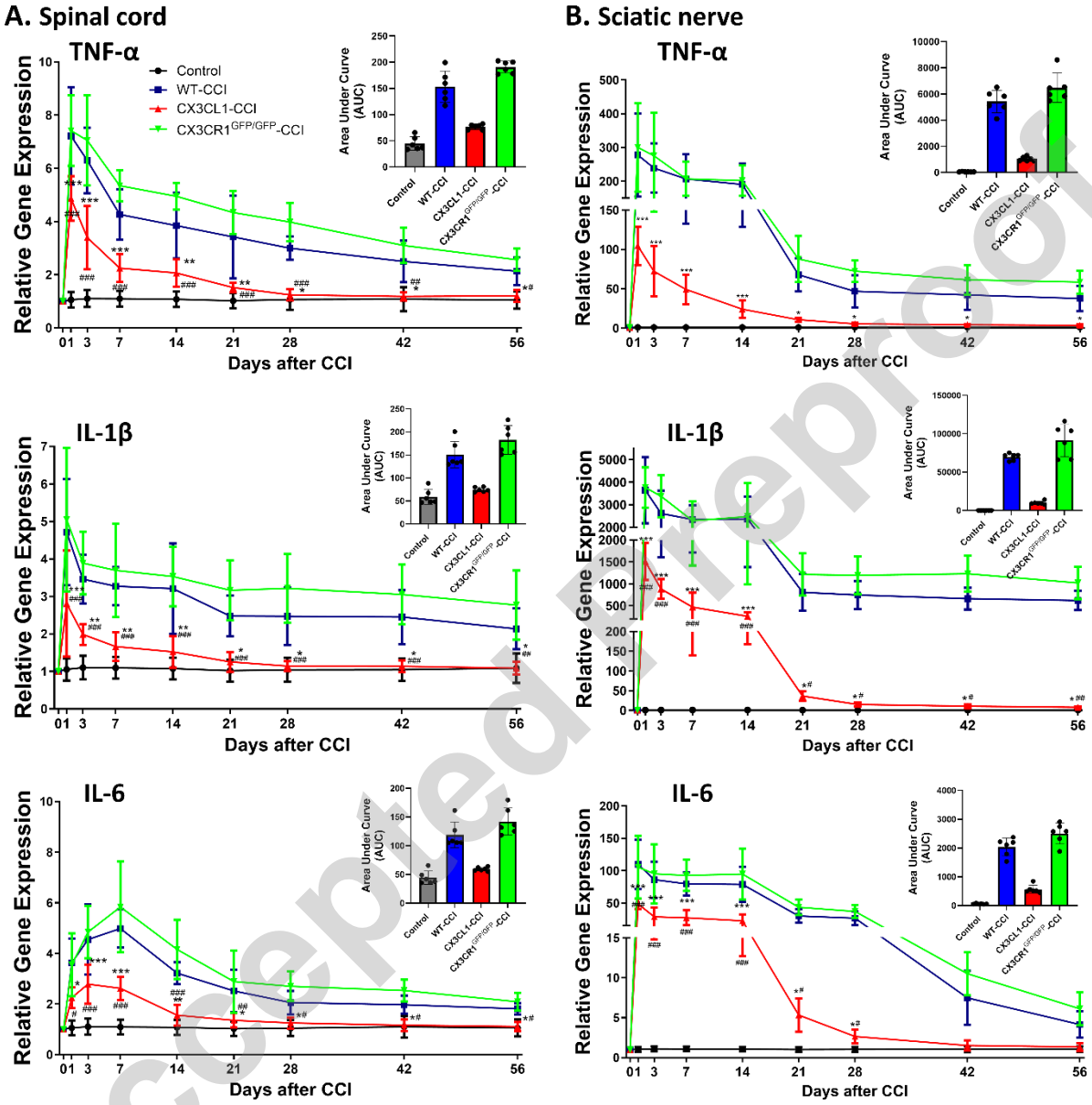

Figure 5

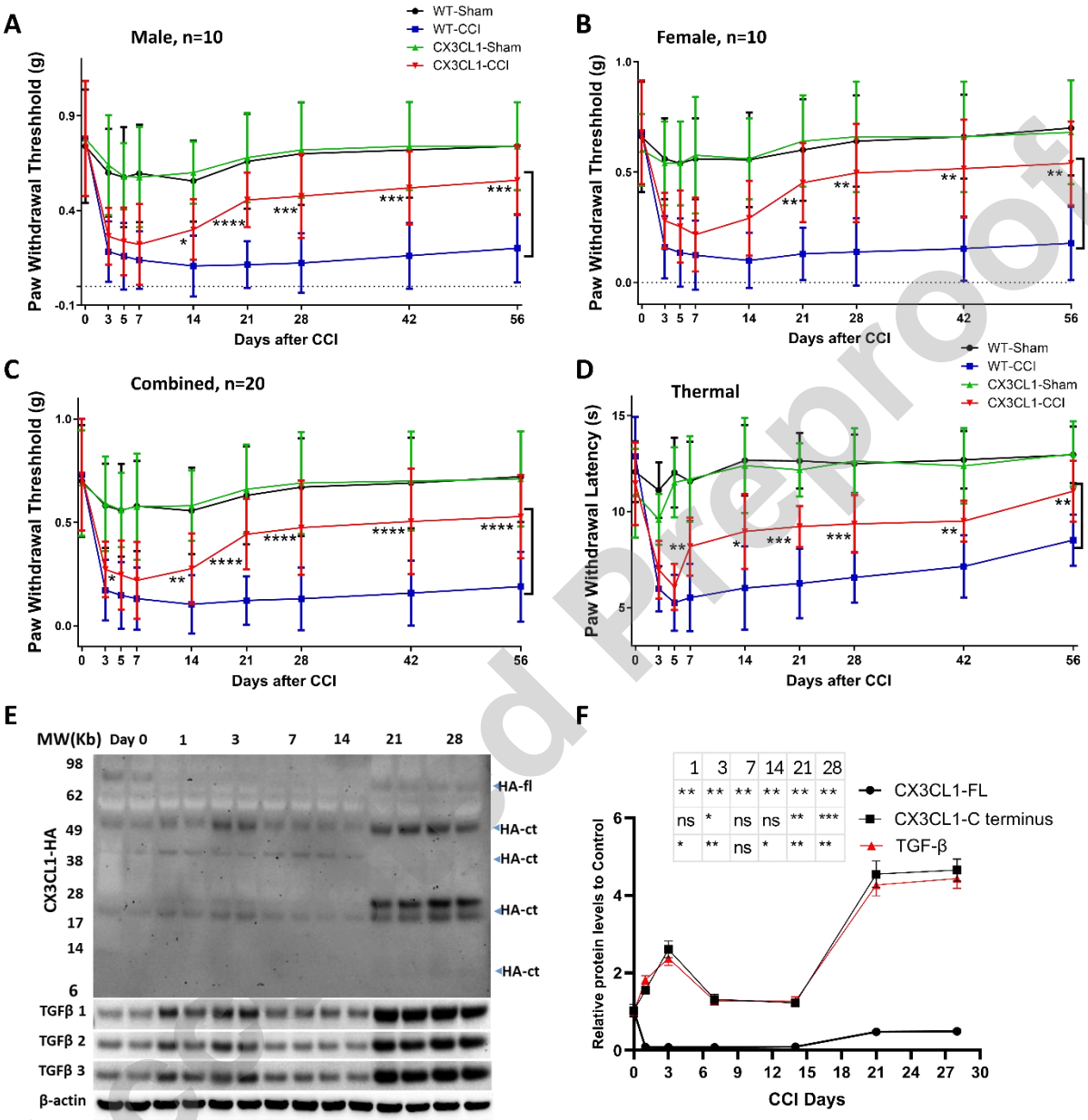

Figure 6A-D

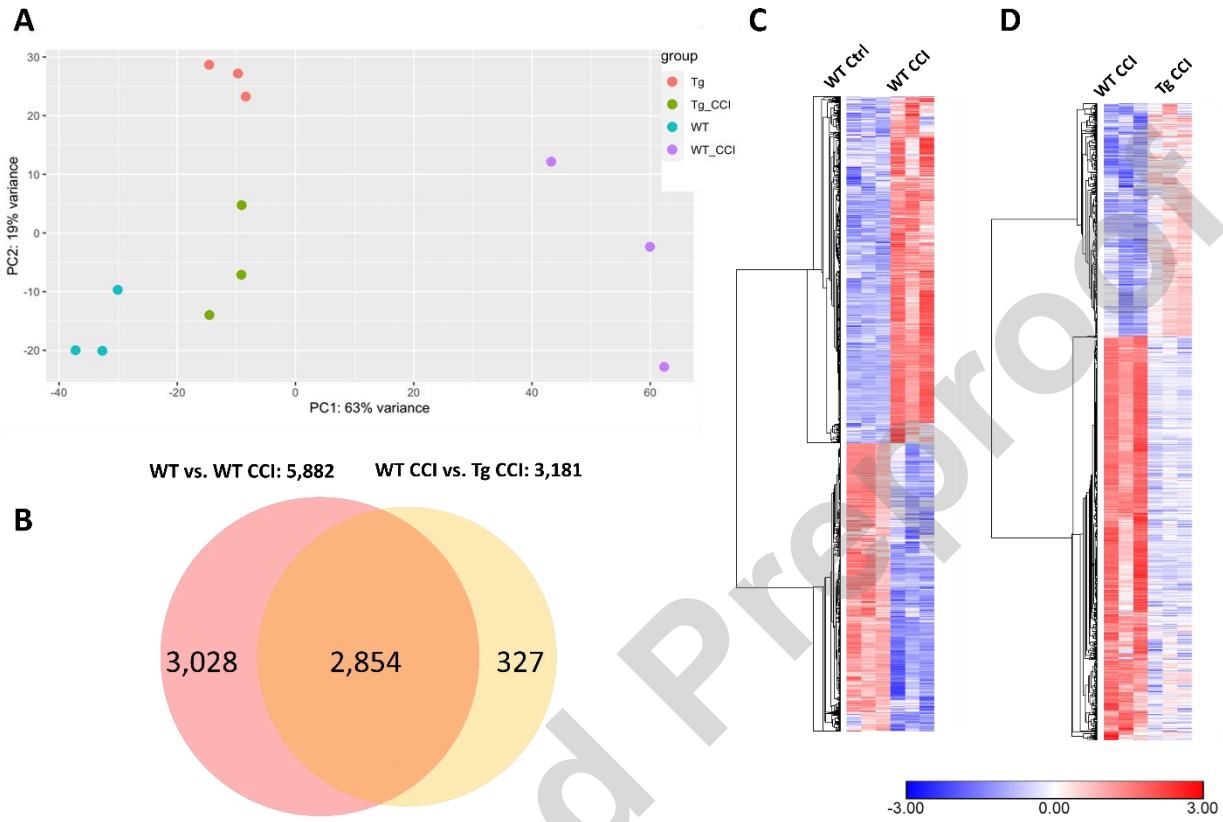

Figure 6E

E

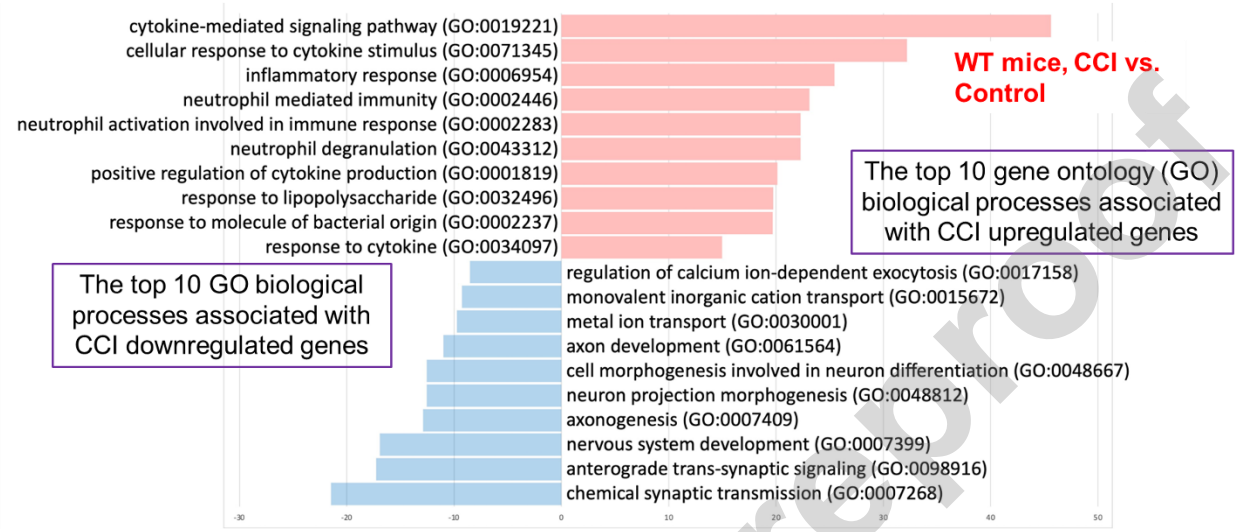

Figure 6E-H

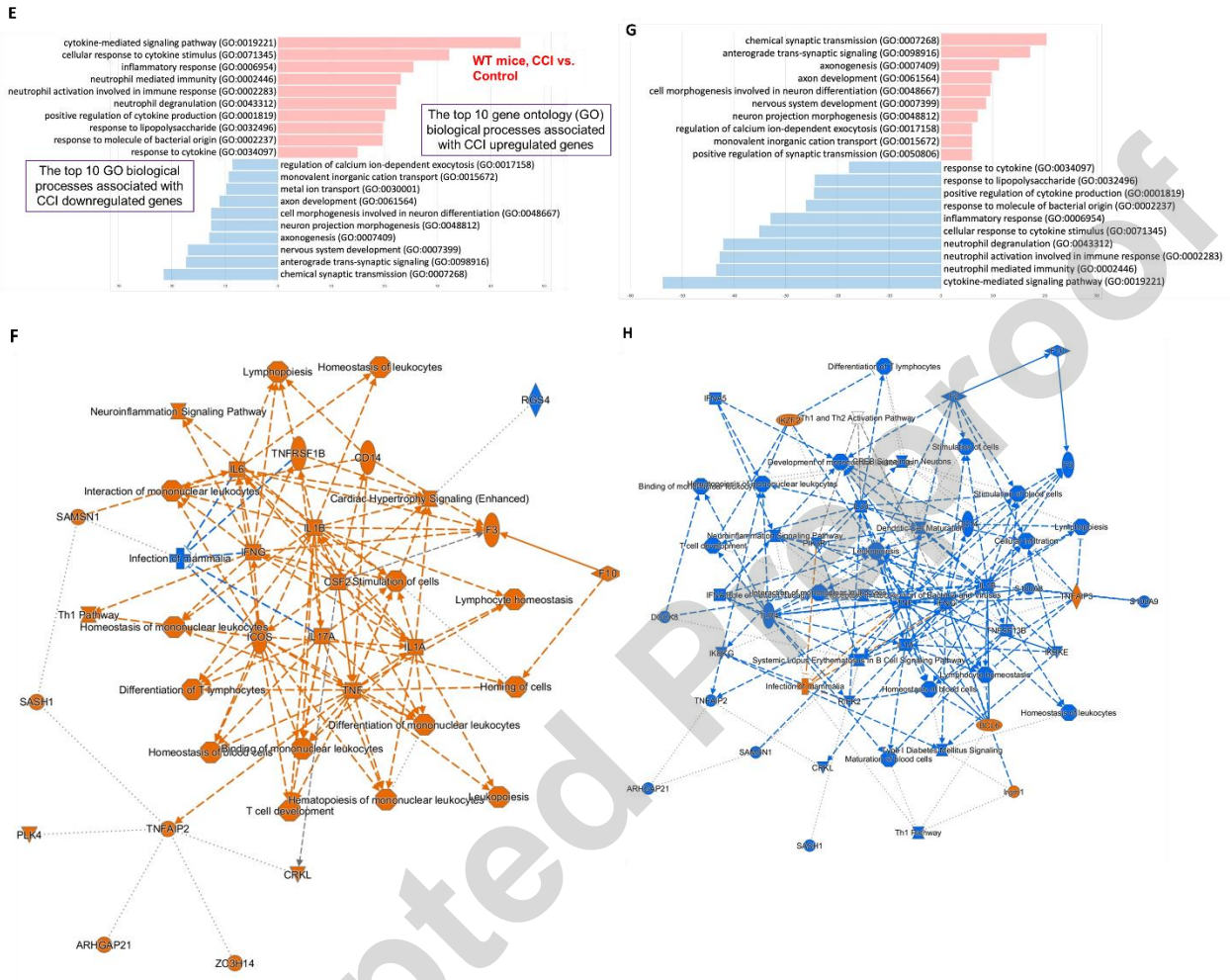

Figure 6F

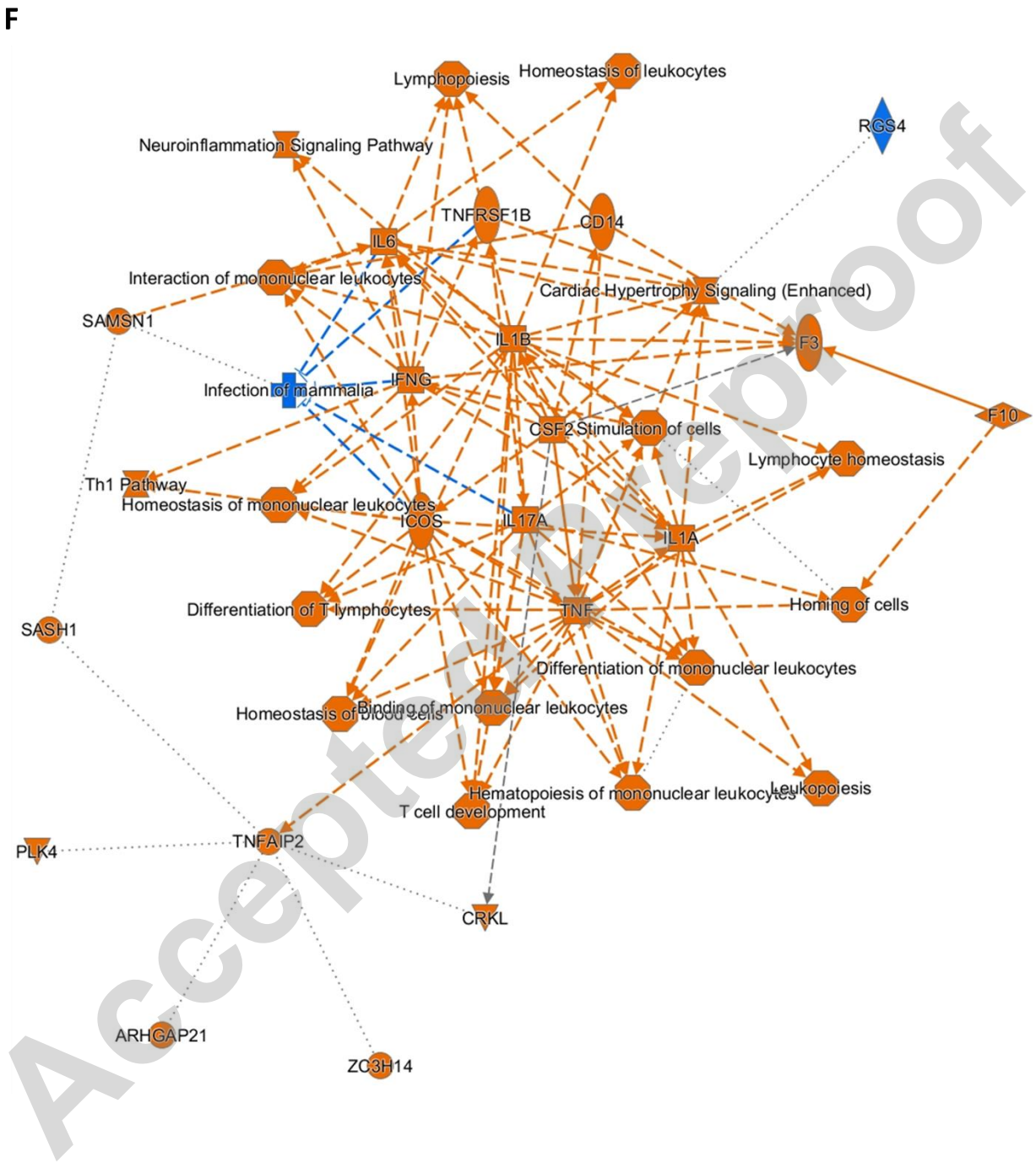

Figure 6G

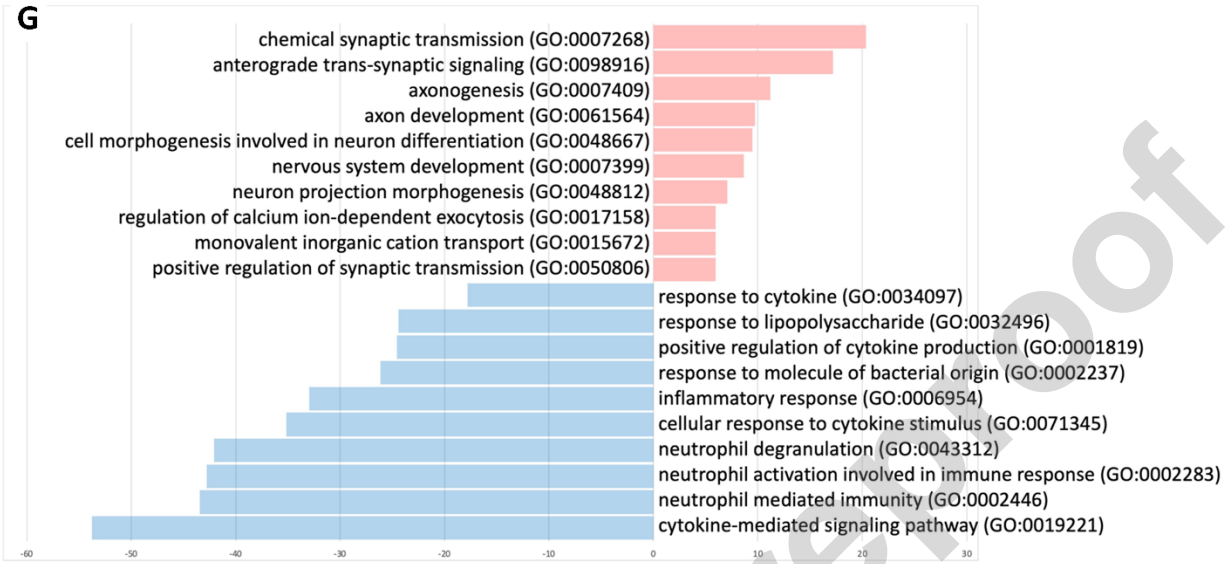

Figure 6H

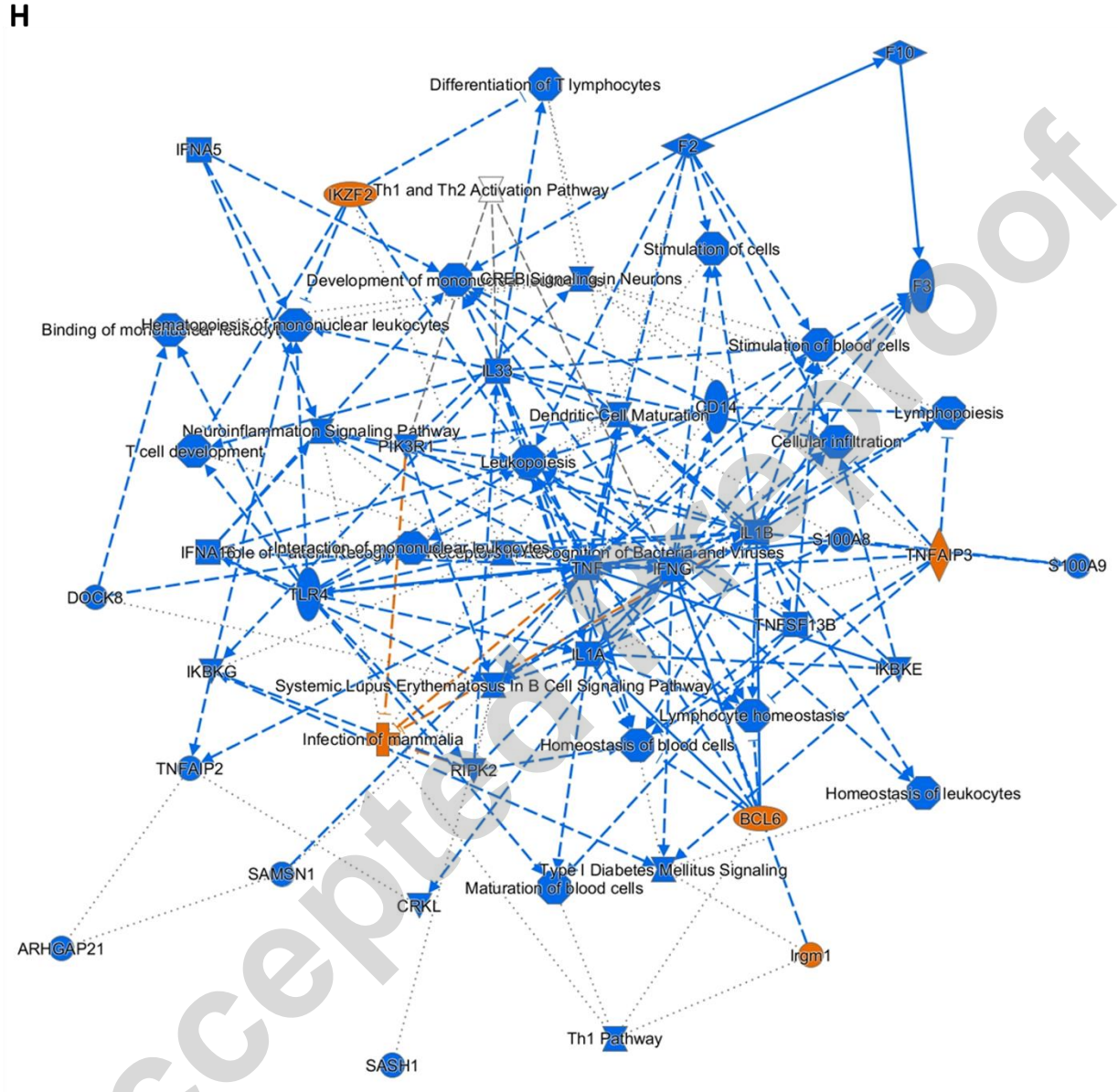

Figure 7A

A

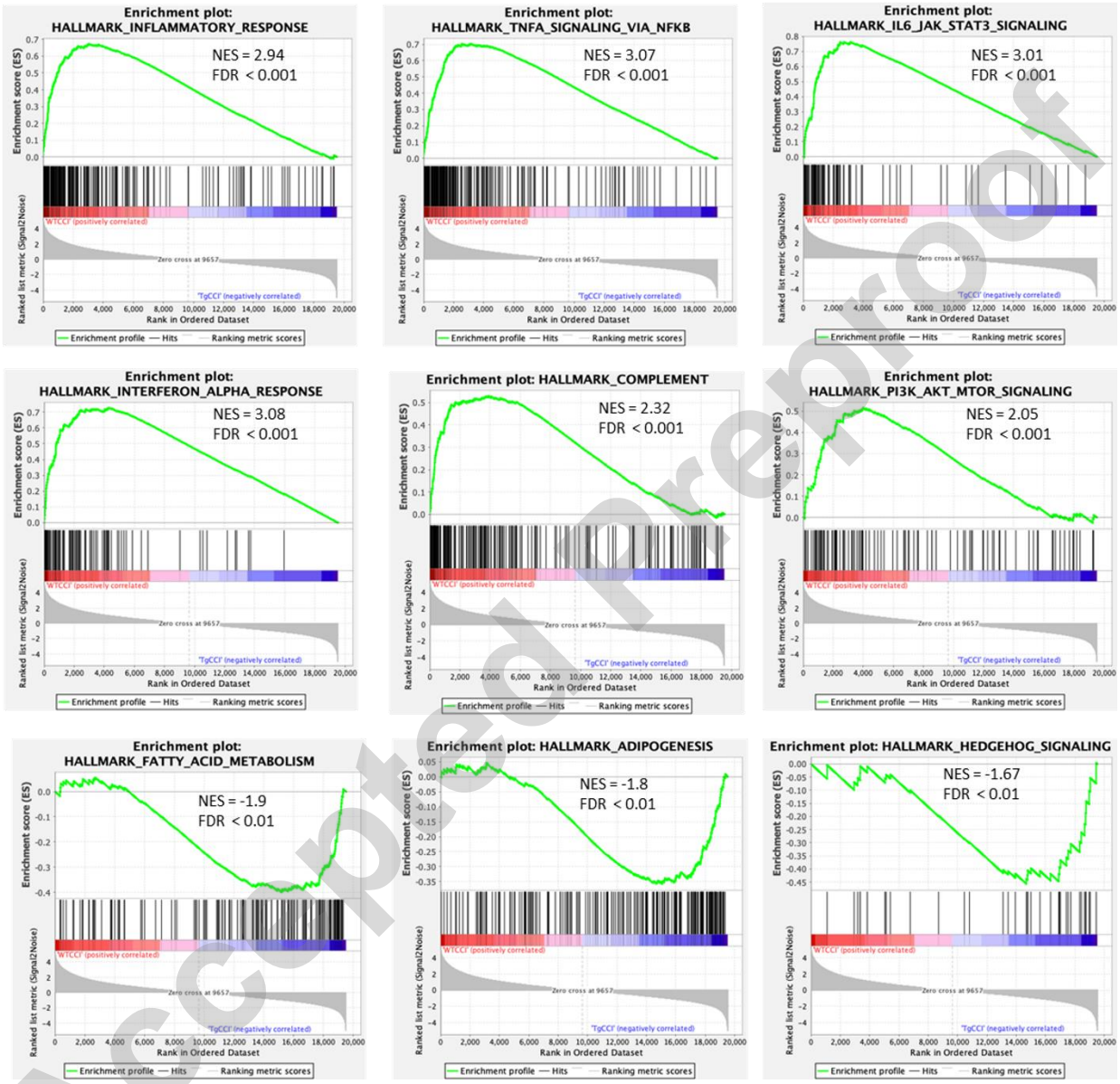

Figure 7B

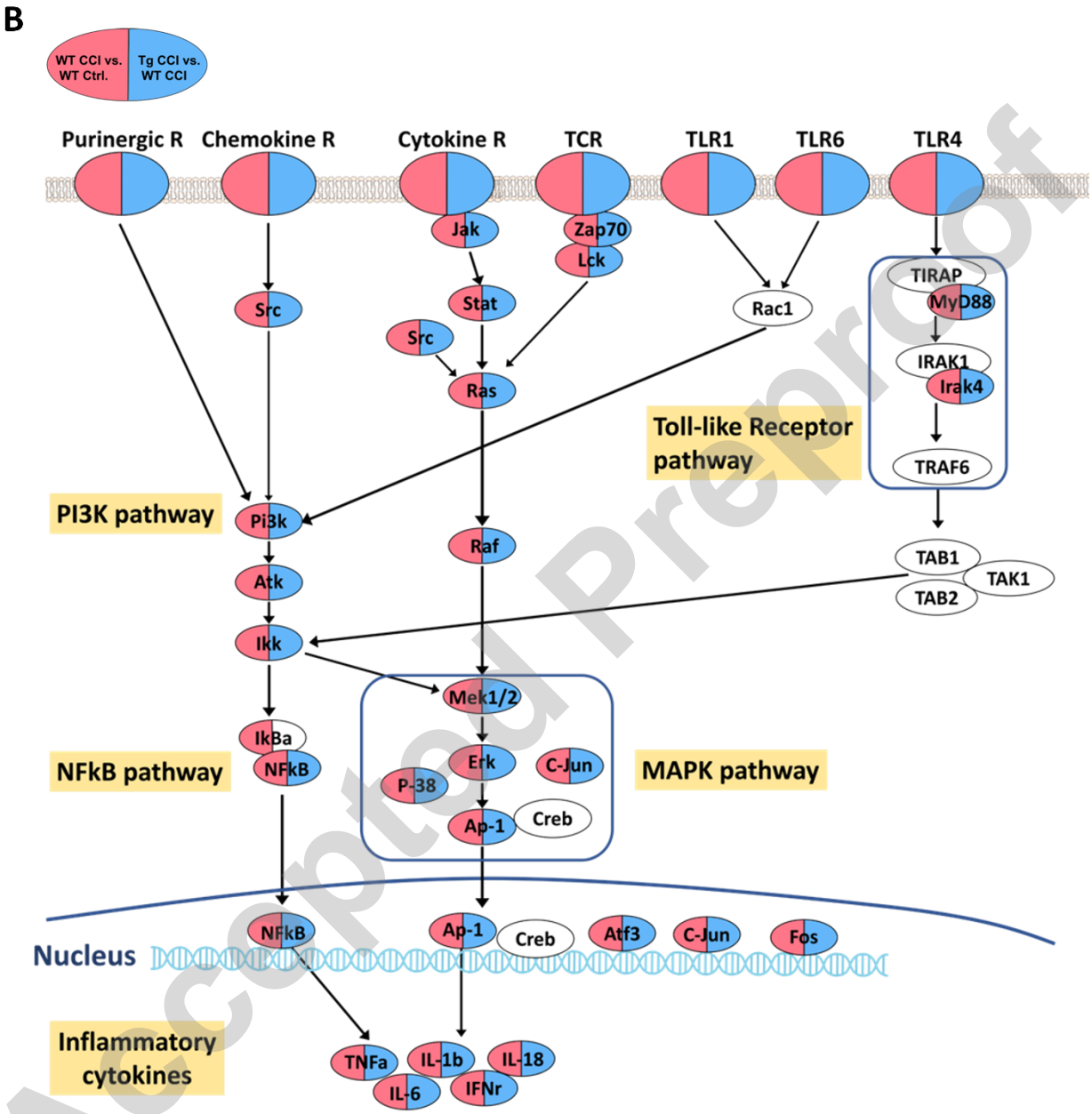

Figure 8A